Facies anatomy of a progradational submarine channelized lobe complex: semi-quantitative analysis of the Ropianka Formation (Campanian–Paleocene) in Hucisko Jawornickie section, Skole Nappe, Polish Carpathians

PIOTR ŁAPCIK

Jagiellonian University, Institute of Geological Sciences, ul. Gronostajowa 3a, PL-30-387 Kraków, Poland.
E-mail: piotr.lapcik@doctoral.uj.edu.pl

ABSTRACT:

Łapcik, P. 2019. Facies anatomy of a progradational submarine channelized lobe complex: semi-quantitative analysis of the Ropianka Formation (Campanian–Paleocene) in Hucisko Jawornickie section, Skole Nappe, Polish Carpathians. *Acta Geologica Polonica*, **69** (1), 111–141. Warszawa.

This study is a detailed lithofacies analysis of the Wiar and Leszczyny members of the deep-marine Ropianka Formation (Campanian–Paleocene) exposed in the Hucisko Jawornickie section of the Skole Nappe, Polish Carpathian Flysch. The sedimentary succession (>400 m thick) represents a channelized lobe complex that prograded at the base of submarine slope. Seven sedimentary facies are recognized as a record of the principal modes of sediment deposition. Based on their stratigraphic grouping and grain-size trends, six facies associations are distinguished as representing specific sub-environments of the depositional system: distributary channels, channel-mouth lobes, channel levees, crevasses and interlobe basin plain with crevasse splays. The individual facies associations are characterized statistically and their internal facies organization is analysed by the method of embedded Markov chains to reveal the time pattern of depositional processes. The environmental changes indicated by the vertical succession of facies associations are attributed to the autogenic processes of the distributary channel shifting within an aggrading lobe area and the lateral switching of depositional lobes. Eustatic influences are likely, but difficult to ascertain with poor biostratigraphic data. The bulk basinward advance of the base-of-slope system was probably due to a pulse of the tectonic narrowing of the synclinal Skole Basin.

Key words: Deep-marine turbidites; Depositional lobes; Submarine channels; Dynamic stratigraphy; Facies analysis; Markov-chain analysis.

INTRODUCTION

Worldwide studies of submarine channel–lobe complexes in base-of-slope settings have shown that these sedimentary systems vary enormously in their dimensions, lithofacies assemblages and stratigraphic architecture (e.g., Heller and Dickinson 1985; Nelson *et al.* 1991; Shanmugam and Moiola 1991; Pickering *et al.* 1995; Galloway 1998; Bouma 2000; Wynn *et al.* 2002; Gardner *et al.* 2003; Prélat *et al.* 2009, 2010; Brunt *et al.* 2013; Bayliss and Pickering 2015a, b; Łapcik 2017; Nemec *et al.* 2018). Inconsistent methods of sedimentological description render case studies difficult to compare, and the classification of these systems into some distinctive categories with predictive facies models remains a formidable task. Generalized non-specific models are superficial, short of informative detail (e.g., Stow and Mayall
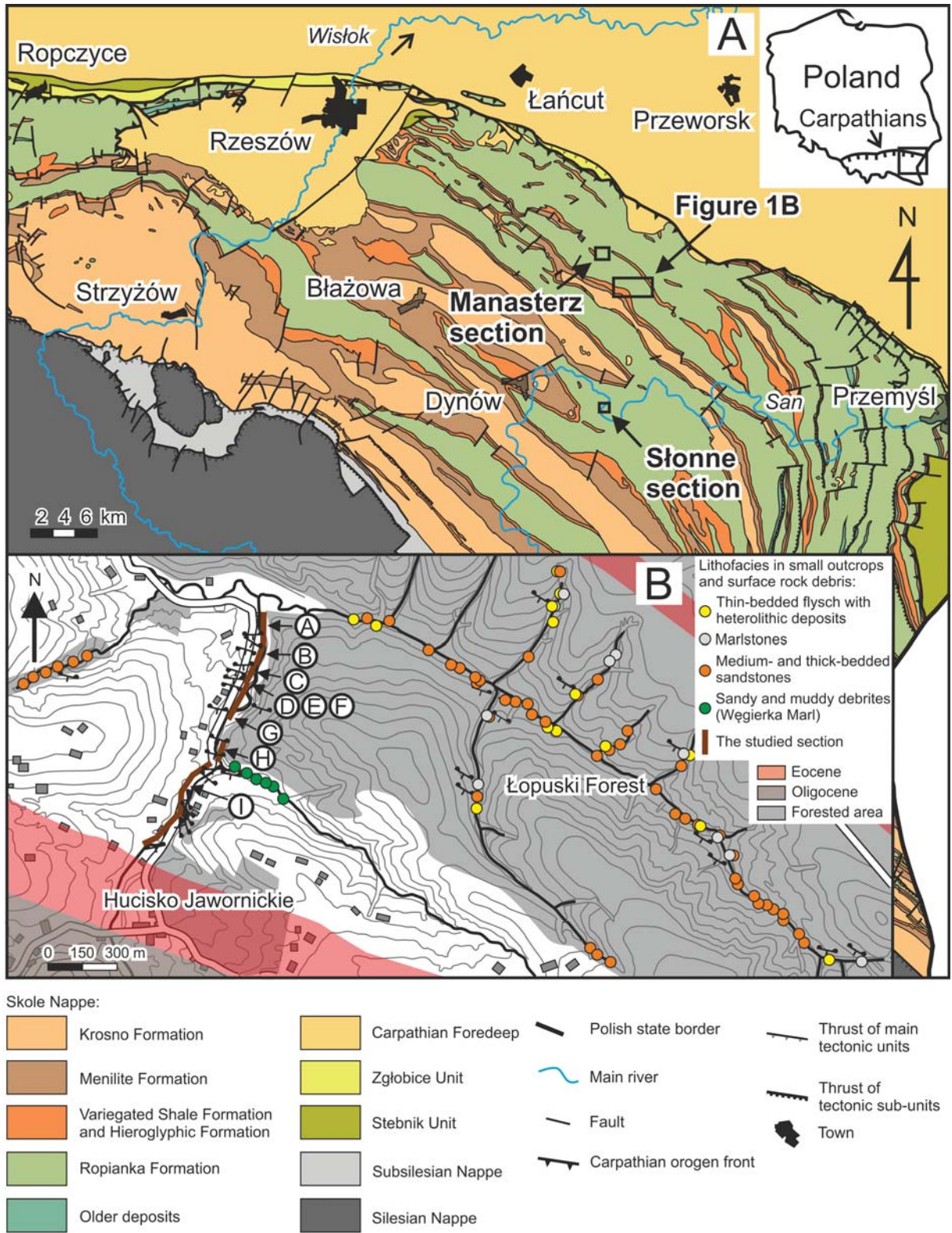
Text-fig. 1. Location of the study area; A – Geological map of the Skole Nappe (compiled from Gucik *et al*. 1980; Jurkiewicz and Woiński 1981; Woiński 1994; and Nescieruk *et al*. 1995). Note the location of present study area and outcrop sections studied by Łapcik (2017, 2018); B – Location of the Hucisko Jawornickie section and small other outcrops of the Ropianka Formation in the study area

2000; Posamentier and Walker 2006), and are of little use as a guide for exploration and reservoir characterization. What is needed is a more consistent and preferably quantitative methodology for the description and synthetic comparison of field cases.

The present case study from the Polish Carpathian Flysch follows the descriptive approach of Łapcik (2017) and uses a semi-quantitative methodology of facies analysis and sedimentological characterization of submarine system, similar as originally postulated by Miall (1973, 1978) for alluvial systems. The subject of this study is the Ropianka Formation (Turonian–Paleocene) of the Skole Nappe, a poorly investigated lithostratigraphic unit up to 1.6 km thick composed of deep-marine sediment gravity-flow deposits. The formation is poorly exposed, with good outcrops limited to river cut-bank sections and rare isolated quarries. Previous sedimentological studies have documented a non-channelized depositional lobe complex in the river San cut-bank section near Słonne (Łapcik 2017) and a large feeder paleochannel in the Manasterz Quarry section (Łapcik 2018) (Text-fig. 1A). The present study from the Hucisko Jawornickie outcrop section (Text-fig. 1A) contributes to an understanding of this formation's palaeoenvironmental jigsaw puzzle by documenting a channelized lobe complex that apparently prograded over the non-channelized distal part of an earlier one at the base of the Skole Basin's northern slope. The sedimentary succession exposed in the Hucisko Jawornickie section is more than 400 m thick and its sedimentological study proceeded in the following main methodological steps:

(i) A detailed bed-by-bed logging of the stratigraphic succession and distinction of its component sedimentary facies as the record of particular depositional processes.

(ii) Analysis of the stratigraphic grouping of sedimentary facies and recognition of their associations as the record of specific sub-environments of the submarine depositional system.

(iii) Quantitative statistical characterization of the individual facies associations in terms of their main descriptive features.

(iv) Analysis of the vertical organization of sedimentary facies (depositional processes) within their individual associations by the stochastic method of Markov chains.

(v) Analysis of the vertical succession of facies associations (sub-environments) as the record of the depositional system's bulk behaviour.

This case study contributes to a better understanding of the Ropianka Formation, while giving a detailed insight into the facies anatomy and sedimentation dynamics of a submarine base-of-slope system. The logging and distinction of facies are based on objective sedimentological criteria, and similarly objective and verifiable are the analytical results of quantitative methods, which jointly provides a reliable and highly informative methodological basis for comparative characterization of such ancient depositional systems. Last, but not least, the study demonstrates that – with appropriate methods – a wealth of valuable sedimentological information can be derived even from poor and isolated outcrops.

GEOLOGICAL SETTING

The Ropianka Formation of Turonian–Paleocene age is one of the major lithostratigraphic units of the Skole Nappe (Text-fig. 1A), subdivided into four members (Text-fig. 2; Kotlarczyk 1978). The deep-marine Skole Basin formed in the Early Cretaceous as the most external of the Carpathian flysch basins (Gucik 1963; Kotlarczyk 1988). After more than 100 Ma of variable deep-water sediment accumulation (Text-fig. 2), the basin was inverted by tectonic contraction and thrust – as the Skole Nappe – onto the Carpathian Foredeep in the early Miocene (Kotlarczyk 1988; Gągała et al. 2012; Ślączka et al. 2012; Kováč et al. 2016). The deposition of the Ropianka Formation was preceded by deposition of black and variegated shales (Cenomanian–Turonian), which accumulated below the local CCD in conditions changing from dysoxic with periodic anoxia to well-oxygenated (Gucik 1963; Bąk 2007; Bąk et al. 2014 and references therein). Similar correlative deposits are known from all the basins of the Polish Outer Carpathians. Tectonic activity and increased sand supply in the Skole Basin then caused depositions of the flysch of Ropianka Formation (Malata and Poprawa 2006; flysch definition sensu Dżułyński and Smith 1964). This flysch succession, up to 1.6 km thick, was deposited at a bathyal depth range around the local CCD (Uchman et al. 2006). The corresponding transport directions, measured in the present-day Skole Nappe, are mainly form the NE, N and NW (Książkiewicz 1962; Bromowicz 1974; Kotlarczyk 1978, 1988).

The Ropianka Formation represents a mixed sand-mud system dominated by siliciclastic sediment, but shows an abundance of marls towards the northerly source area, particularly in the eastern part of the Skole Nappe (Burzewski 1966; Kotlarczyk 1978, 1988; Geroch et al. 1979; Leszczyński et al. 1995; Leszczyński 2003, 2004; Kędzierski and Leszczyński
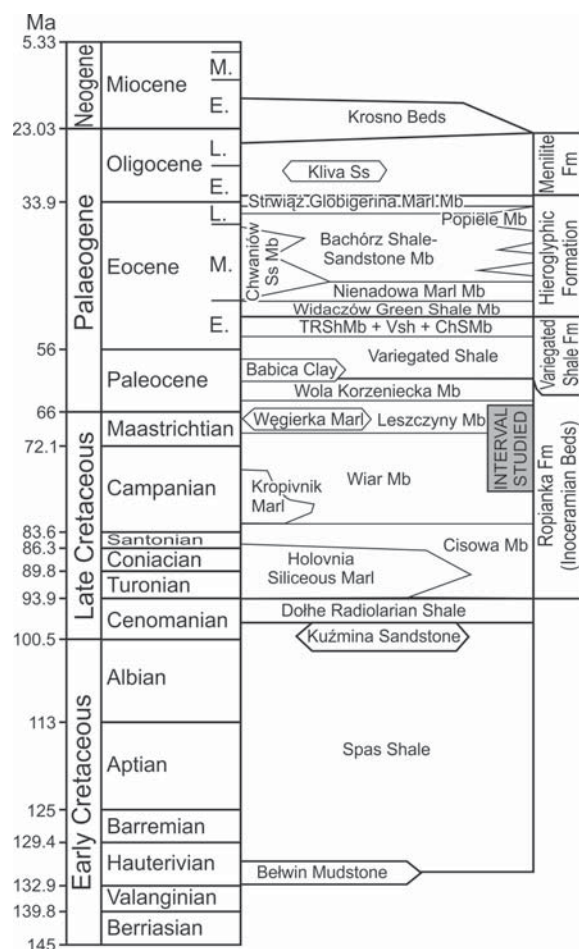
Text-fig. 2. Stratigraphic scheme of the Skole Nappe, based on Kotlarczyk (1988), Rajchel (1990), Rajchel and Uchman (1998) and Ślączka and Kaminski (1998), with modifications by Gedl (1999) and Kotlarczyk *et al.* (2006). The time scale is according to Gradstein *et al.* (2012). Abbreviations: TRSh Mb – Trójca Red Shale Member; VSh – Variegated Shale; and ChS Mb – Chmielnik Stripy Sandstone Member

2013). Exotic components and heavy-mineral assemblages in sandstones indicate a varied crystalline rock suite of the northern hinterland (Salata and Uchman 2013; Salata 2014a, b; Łapcik *et al.* 2016 and references therein). The zone of marl sedimentation between the siliciclastic source and similarly siliciclastic mass-flow system of the Ropianka Formation suggests a slope zone of the Skole Basin and an intra-basinal origin of carbonate mud. In the outcrop of thrust-folded Skole Nappe (Text-fig. 1A), the marlstones occur mainly as wedges in the lower parts of the Cisowa, Wiar and Leszczyny members of the Ropianka Formation (Text-fig. 2), which may indicate basinward slope advances accompanied by

base-of-slope sandy sedimentation. At its top, the Ropianka Formation passes into the Paleocene–Eocene Variegated Shale Formation (Text-fig. 2) deposited below the local CCD in variable oxygenation conditions (Rajchel 1990; Leszczyński and Uchman 1991; Barwicz-Piskorz and Rajchel 2012; Olszewska and Szydło 2017), which suggests bulk deepening of the basin and drowning of its sediment-supplying hinterland.

The study area near the village of Hucisko Jawornickie (Text-fig. 1A) is located about 3 km to the SE from the Manasterz Quarry section studied by Łapcik (2018), but the two localities are in different adjacent thrust sheets (cf. Wdowiarz 1949) and their stratigraphic correlation is uncertain. The outcrops studied are in the stream banks to the north of Hucisko Jawornickie and in the Łopuski Forest to the northeast (Text-fig. 1B). The best exposed and longest section north of Hucisko Jawornickie shows the Wiar and Leszczyny members of the Ropianka Formation and the overlying Variegated Shale Formation (Text-fig. 2), although their exact boundary there is unexposed. According to regional literature, the topmost part of the Ropianka Formation in the Hucisko Jawornickie section (its segment I, Text-fig. 1B) represents the Węgierka Marl (Text-fig. 2), known also as the Baculites Marl (Burzewski 1966; Bromowicz 1974; Kotlarczyk 1978).

MATERIAL, METHODS AND TERMINOLOGY

The main part of data for the present study are from a detailed logging of the Hucisko Jawornickie outcrop section, showing a stratigraphic thickness of more than 400 m. The rocks are tectonically deformed and steeply inclined towards the SW, which means that the section is stratigraphically oblique, drifting away from the basin margin in the upward direction. The outcrop section is discontinuous, with some of its parts covered by vegetation and modern fluvial sediments. The section has been subdivided in a stratigraphic order into segments A to I (Text-fig. 1B), with segment B as a stratigraphic equivalent of segment A, measured on the opposite limb of the same syncline. Supplementary observations are from the small isolated outcrops and loose rock debris in the areas to the west and east of the Hucisko Jawronickie section (Text-fig. 1B), although these data on lithofacies variability along the depositional strike are difficult to correlate with the logged outcrop section.

The descriptive sedimentological terminology is after Harms *et al.* (1975) and Collinson *et al.* (2006).

Bed thickness categories are after Nichols (2009), with very thin (<1 cm), thin (1–10 cm), medium (10–30 cm), thick (30–100 cm) and very thick (>100 cm) classes. Statistical terminology and methods are after Davis (2002).

Sedimentary facies are basic types of deposits distinguished on the descriptive basis of their bulk macroscopic characteristics (Walker 1984). In the case of episodic 'event sedimentation' (*sensu* Dott 1983), as in a flysch succession, the distinction of facies pertains to the products of individual sedimentary-gravity flows and inter-flow episodes of background sedimentation (e.g., Janbu *et al.* 2007). Differing assemblages of spatially and temporarily related sedimentary facies are distinguished as facies associations and considered to represent specific parts (sub-environments) of the sedimentary system (e.g., Stow and Mayall 2000; Mulder *et al.* 2011; Shanmugam 2016a). They are given interpretive genetic labels, but their descriptions are separated from interpretations in the text.

SEDIMENTARY FACIES

Seven sedimentary facies are distinguished in the studied succession, ranging from granule conglomerates and sandstones to mudstones and marlstones, and are labelled F1 to F7 in the sedimentological log (Text-fig. 3). Sedimentary facies are distinguished based on the texture, grain size trend, mud content, bed thickness, sedimentary structures and petrographic composition of deposits. Sandstones are quartzose arenites, variably calcareous and mainly whitish grey or yellowish to rusty orange in colour. Some sandstone beds are greenish due to a high content of glauconite. Most sandstone beds are poorly cemented, as is typical of the Ropianka Formation (Bromowicz 1974). In addition to quartz, the sandstones contain grains of muscovite, biotite, feldspar, pyrite, glauconite, coal and plant detritus, as well as fragments of siliceous rocks, greenschist, grey mudstone and agglutinated foraminifer tests. Conglomerates are subordinate, fine-grained and dominated by quartz.

**Facies F1: Graded massive conglomerate and sandstone with stratified or banded top**

Description: This facies occurs as beds of graded coarse- to fine-grained sandstone or granule conglomerate graded to sandstone. Beds are 4 to 195 cm in thickness and mainly tabular on the outcrop scale, with sharp erosional bases, load features and rarely exposed sole marks. These graded beds are mainly or entirely massive, macroscopically non-stratified (Text-fig. 4A–C). Some beds contain flat-lying intraformational clasts of mudstone, siltstone, marlstone and coal, most often in the basal and/or top part of massive bed. Intraclasts are up to 17 x 6 cm in size and are lithologically similar to facies F4, F5 and F6 (described farther in the text). Exotic pebble-sized clasts of schist, igneous and volcanic rocks, limestone, sandstone and siliceous rocks occur in the basal part of beds. Some beds are multiple, amalgamated, as indicated by erosional surfaces with an abrupt increase is grain size.

The top part of the graded massive beds often shows planar parallel stratification and ripple cross-lamination, occasionally convoluted, and a siltstone to mudstone capping with 'wispy' discontinuous lamination (Text-fig. 4B). Many beds show a significant grain-size decrease and mud content increase at the transition from their graded massive division to laminated top division. The laminated division is typically much thinner than the massive division (Text-fig. 4A), but is occasionally of similar or greater relative thickness (Text-fig. 4B). The top of the laminated division is only rarely disturbed by bioturbation.

Some beds of facies F1 show dark isolated bands, 0.5–5 cm thick and rich in mud and coalified plant detritus, which occur at various heights within the massive graded division or form its capping instead of a laminated division. In the latter case, the banded division (*sensu* Lowe and Guy 2000) consists of thin dark bands of massive sand alternating with 'clean' bands of laminated sand, often loaded (Text-fig. 4C). These bands have comparable thicknesses or either type may dominate, even in portions of one banded division. The sandstone below banded division or beneath an isolated band in massive division commonly shows dewatering structures, and the bands in such cases are hydroplastically deformed. Similar banded divisions were observed by Łapcik (2017) in the turbidites of the Ropianka Formation in the Słonne section.

Interpretation: Facies F1 is interpreted as deposits of high-density turbiditic currents (*sensu* Lowe 1982). The graded massive division represents a phase of rapid, non-tractional dumping of coarse sediment suspension from a highly concentrated turbulent flow (turbidite division A of Bouma 1962; division S_3 of Lowe 1982). The overlying laminated division represents tractional deposition from the remaining, lower-density phase of the current (divisions B–D of Bouma 1962; division T_t of Lowe 1982), with possible brief episodes of bypass and substrate reworking (e.g., Sumner *et al.* 2008; Talling *et al.* 2012). Such a pattern of deposition is generally attributed
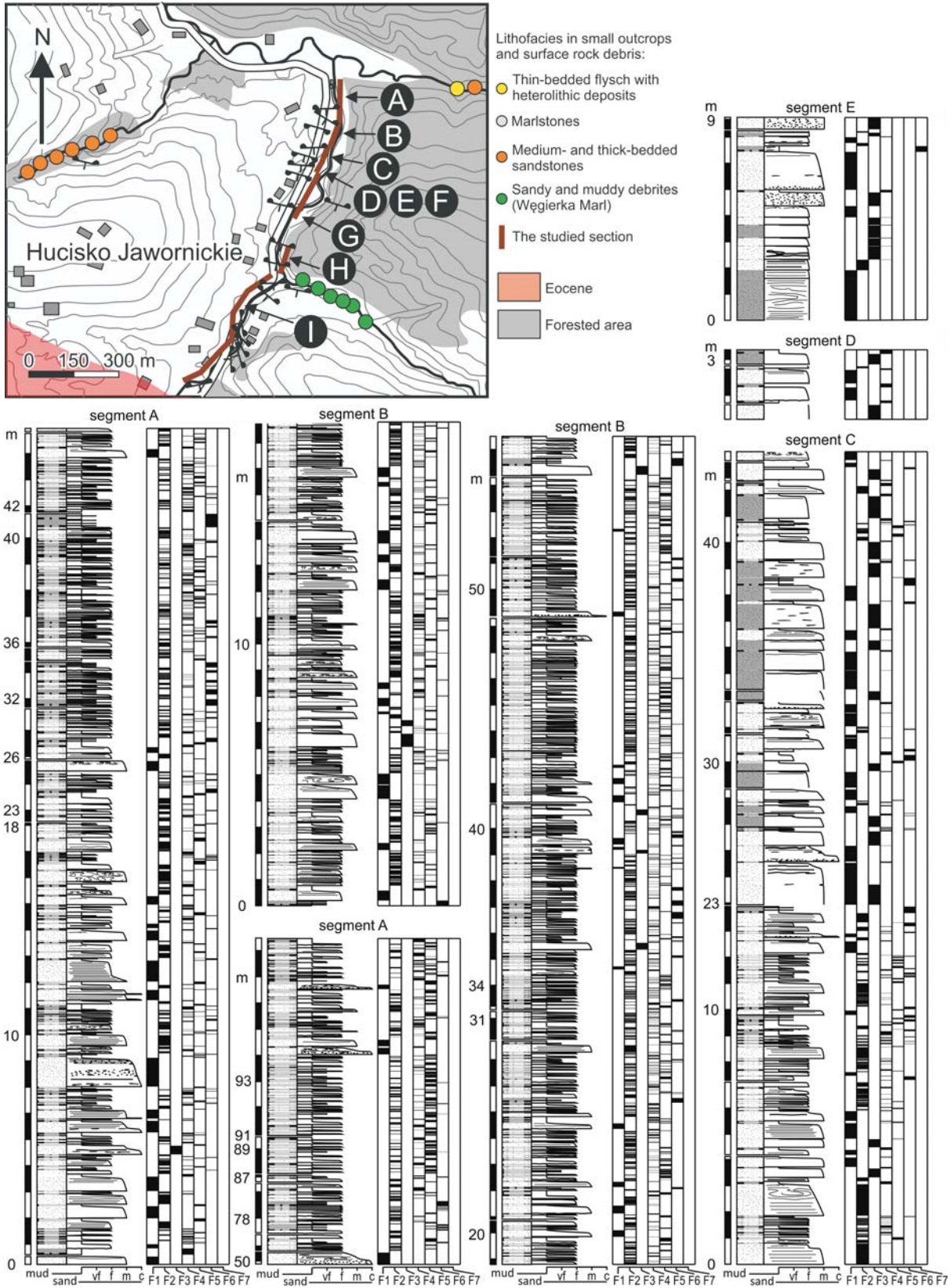
Text-fig. 3 (continued on p. 7)
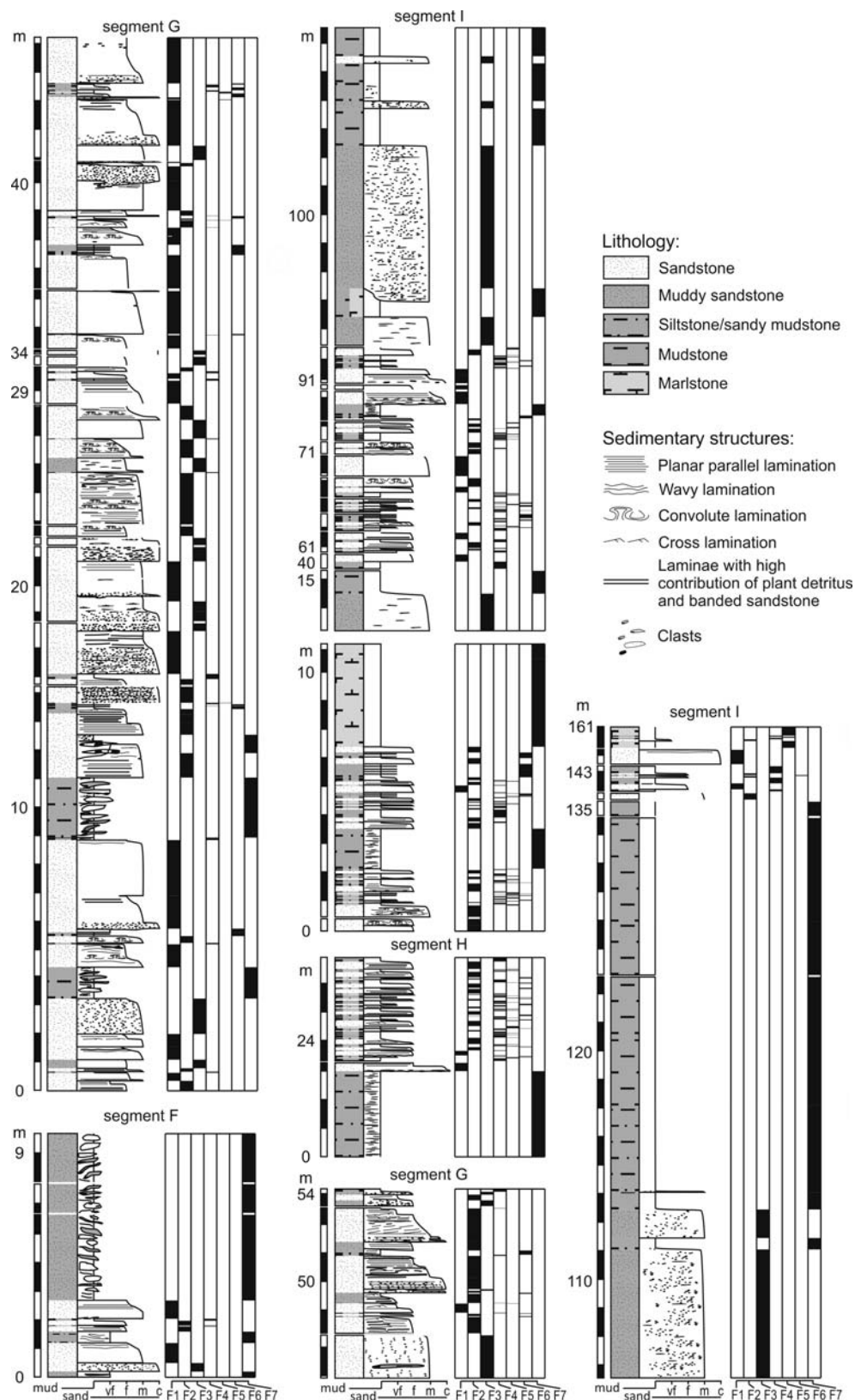
Text-fig. 3. Sedimentological log of the Ropianka Formation in the Hucisko Jawornickie section, with the distinction of sedimentary facies (see F1–F7 in the chequer plot at the log right-hand margin). The inset map shows the location of individual log segments A–I
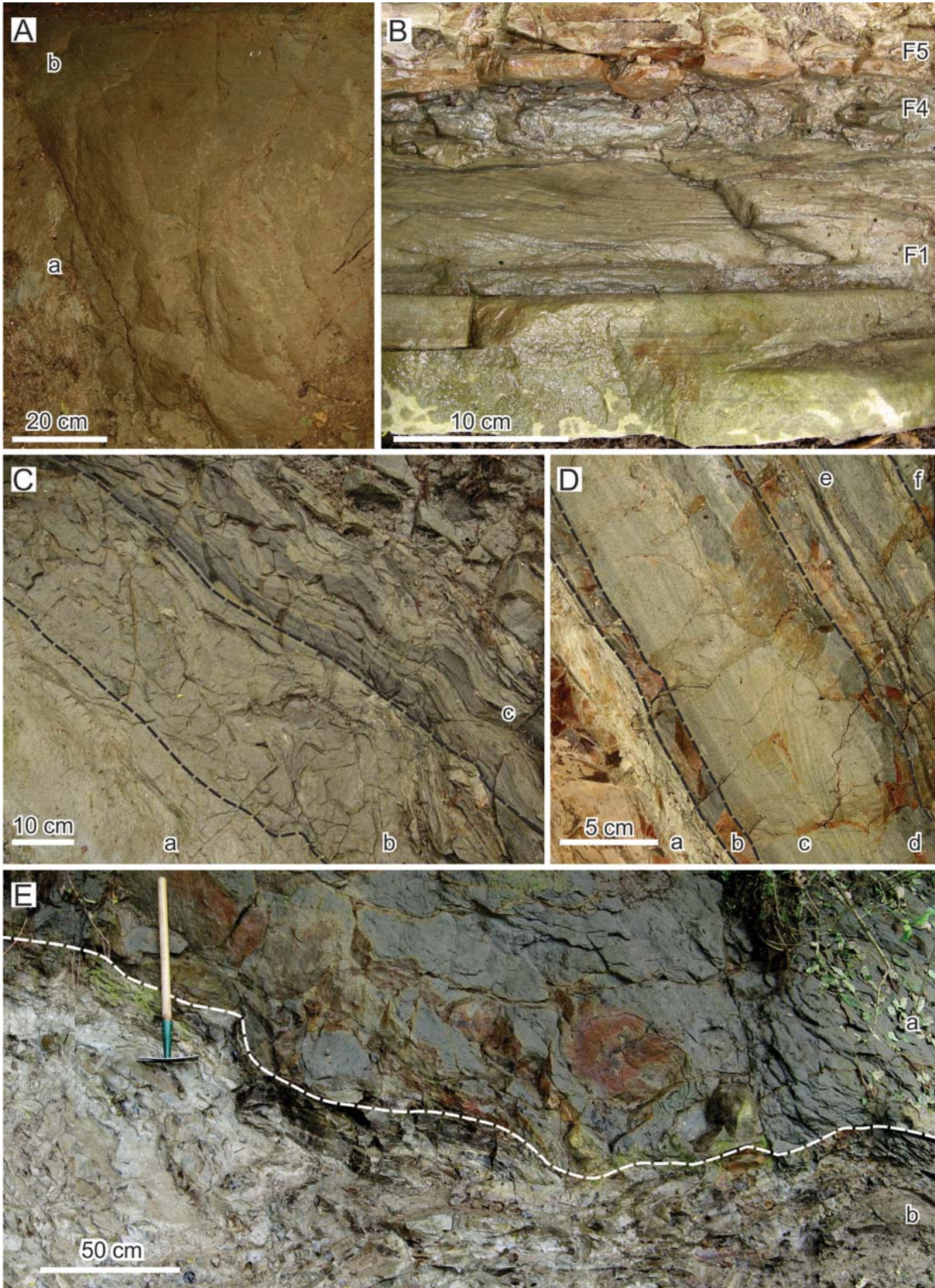
to the waning of a 'classical', surge-type turbidity current (Bouma 1962; Piper 1978; Stow and Bowen 1978, 1980; Lowe 1982, 1988; McCave and Jones 1988; Best and Bridge 1992; Leclair and Arnot 2005; Sumner *et al.* 2008; Talling *et al.* 2012). However, it cannot be precluded that at least some of the thicker beds of facies F1 were deposited by quasi-steady, 'sustained' (long duration) turbidity currents (see Kneller and Branney 1995; Baas 2004; Leclair and Arnot, 2005). The isolated dark sand bands enriched in mud and coaly detritus within the massive division indicate, indeed, some internal flow pulses, with the mode of deposition perhaps intermediate between turbidity current and debris flow (cf. Lowe *et al.* 2003; Haughton *et al.* 2009). Likewise, the overlying banded division observed in beds indicates rhythmic pulses of deposition from a sustained quasi-steady flow, similar to the flow mode referred to as 'slurry flow' by Lowe and Guy (2000). This flow mode would involve repetitive auto-cyclic formation and *en masse* freezing of cohesive traction carpets (in contrast to the non-cohesive traction carpets of Lowe 1982) due to the settling of flocculated mud and entrapped coaly detritus, with the intervening episodes of tractional sand deposition. The bands in facies F1 are in the thickness range of the meso- (M_{2C}) and micro-banding (M_5) of Lowe and Guy (2000), whereas the massive, dish-structured and wispy-laminated deposits underlying the banded divisions might correspond, respectively, to the divisions M_1, M_4 and M_3 of Lowe and Guy (2000).

Last, but not least, the massive lower division in some of the beds of facies F1 shows little or no macroscopically recognizable grading. It may thus be interpreted as a co-genetic sandy debrite (cf. Strzeboński 2015; Shanmugam 2016b) – representing either a relic of the turbidity current's parental debris flow or an inertial debris flow spawned en route by the current as a 'moving bed' due to excessive bedload concentration (cf. Postma et al. 1988; Talling 2013).

Facies F2: Stratified sandstone and conglomerate

Description: Facies F2 occurs as beds of coarse- to very fine-grained sandstone and granule to pebble conglomerate, 1 to 160 cm in thickness. Beds are mainly tabular on the limited outcrop scale, but the thinner ones, up to a few centimetres, tend to have uneven thicknesses with occasional lateral pinch-outs. Bed bases are invariably sharp, with sole marks including trace fossils as well as flute and groove marks. Bioglyphs and mechanoglyphs co-occur, but one type of sole marks seems to dominate in particular parts of the sedimentary succession. Sedimentary structures include planar parallel stratification, ripple cross-lamination (occasionally with climbing ripples), convolute lamination, water-escape features and mud-draped wavy lamination (Text-fig. 4D). The beds of facies F2 thus resemble the laminated and banded top divisions of facies F1 beds, but lack any related lower massive division. Most beds show macroscopic normal grading and the thicker ones are sparsely capped with a laminated siltstone and mudstone. Rare intraformational and exotic clasts, similar as in facies F1, occur scattered in the basal part of some beds. Trace fossils include *Scolicia* isp., *Thalassinoides* isp. and *Ophiomorpha* isp., which occur as hypichnia and endichnia in thin beds.

Interpretation: Facies F2 represents deposits of low-density turbiditic currents (*sensu* Lowe 1982), with a fully tractional deposition and muddy capping as in the Bouma (1962) turbidites T_{BCDE} and T_{CDE} (see also Best and Bridge 1992; Leclair and Arnot 2005; Talling *et al.* 2012). However, the rate of bed aggradation varied and was highly unsteady. Mud-draped wavy lamination indicates discrete pulses of weak tractional transport (Reineck and Singh 1980). Climbing-ripple cross-lamination implies flow phases with a high rate of suspension fallout (Ashley *et al.* 1982). Water-escape structures indicate rapid sediment deposition (Collinson *et al.* 2006), whereas banded divisions suggest transient phases of 'slurry flow' (*sensu* Lowe and Guy 2000).

Within the general concept of turbidity-current evolution (Mulder and Alexander 2001), facies F2 may be considered a downstream equivalent of facies F1 for their parental flows in the depositional system, while it should also be kept in mind that the variation of bed thicknesses and grain size indicates flows with variable volumes and runout distances.

← Text-fig. 4. Outcrop examples of facies F1, F2, F3 and F4; A – Sandstone bed of facies F1 with thick massive division (a) capped by much thinner planar parallel-stratified division (b); B – Sandstone bed of facies F1 with Bouma-type pattern of divisions T_{ABCDE}, capped with a thin mudstone of facies F4 overlain by marlstone of facies F5; C – Massive sandstone bed of facies F1 (a) with mud-richer, darker middle part containing clasts of mudstone, marlstone and laminated siltstone (b); its cap is a banded sandstone division with bands of 'clean' parallel-stratified sand, partly loaded, and dark bands rich in mud and coalified plant detritus (c); D – Marlstone bed of facies F5 (a) overlain by mudstone facies F4 (b), slightly erosional sandstone bed of facies F2 with planar parallel stratification and ripple cross-lamination (c), another mudstone layer of facies 4 (d), and a heterolithic deposit of facies F6 (e) capped with mudstone facies F4 (f); E – Uneven boundary between dark muddy sandstone of facies F3 with scattered mudclasts and quartz granules (a) and the underlying mudstone-marlstone debrite of facies F7 (b)

Facies F3: Non-graded or slightly inverse-graded massive sandstone

Description: Facies F3 consists of fine- to coarse-grained sandstone beds with thicknesses of 4 and 500 cm (Text-fig. 4E). The thin beds are few and are apparently erosional relics of thicker ones. Most beds are darker, richer in mud than the sandstone beds of facies F1 and F2. The lower and upper bed boundaries are sharp, flat or uneven (Text-fig. 4E), lacking sole marks. The sandstone beds are massive (non-stratified) and macroscopically non-graded or slightly coarse-tail inverse-graded. They contain scattered or patchily distributed coarse sand grains, quartz pebbles, coalified plant detritus, and intraformational clasts of mudstone, marlstone and siltstone. Thick beds contain mudclasts up to 72 cm in length. Some beds are capped with a thin layer of finer-grained sandstone showing planar or wavy parallel stratification and/or ripple cross-lamination.

Interpretation: The beds of facies F3 lack evidence of deposition from turbulent flows – such as normal grading and stratification – and are interpreted as deposits of slightly cohesive to non-cohesive sandy debris flows (cf. Shanmugham 2006, 2016b; Breien *et al.* 2010; Talling *et al.* 2012; Talling 2013; Strzeboński 2015). The non-graded beds with randomly scattered outsized clasts suggest slow-moving debris flows with a limited internal shearing (frictional regime *sensu* Drake 1990). The weak, coarse-tail inverse grading of some beds is due to the lack or sparsity of coarse clasts in the bed's lower part, which indicates slightly faster debris flows with a thicker basal shearing zone (see Nemec and Postma 1991). Only some beds have a thin finer-grained stratified capping, which supports the notion of low-speed debris flows with little or no interface turbulent entrainment of sediment by ambient water (cf. Nemec *et al.* 1984).

Facies F4: Mudstone

Description: This facies comprises mudstone beds, 1 to 25 cm thick and grey, greenish or brownish in colour (Text-fig. 4B–D). These beds have gradational, rarely sharp, lower boundaries and most often are sharply overlain by sandstone facies (Text-fig. 5A). Mudstone is mainly massive and variably calcareous, with an admixture of muscovite, pyrite, glauconite, coalified plant detritus, as well as dispersed quartz grains of very fine sand and silt. The thicker beds are partly interlaminated with silt and/or very fine sand. Biogenic component is mainly tests of benthic agglutinated and planktic calcareous foraminifers. The dark colour and weathered outcrop surface of mudstone makes bioturbation structures difficult to recognize in the field, but cut samples show *Chondrites* isp. and *Planolites* isp. The beds of facies F4 alternate with all the other facies in the studied succession, although the bulk thickness contribution of this facies is minor.

Interpretation: This mudstone facies is interpreted as deposits of a 'background' sedimentation above or close to the local lysocline. Macroscopic distinction between pelagic, hemipelagic and turbiditic mudstones is generally difficult. The mudstones of facies F4 are siliciclastic, but are also variably calcareous, which suggests a mixed hemipelagic and pelagic sedimentation. Mudstone beds richer in biogenic calcareous component may thus indicate a relatively higher contribution of pelagic sedimentation. Mudstone beds with a marked admixture of silt and sand or interlaminated with these coarser components, especially where overlying turbidite beds, are thought to represent deposition from the dilute low-density tails of turbidity currents (turbidites T_{DE} of Bouma 1962; see also Stow and Bowen 1978, 1980; McCave and Jones 1988; Talling *et al.* 2012). It is well known from laboratory experiments (e.g., Alexander and Morris 1994; Alexander and Mulder 2002) that the mobile trailing cloud of dilute suspension can spread far beyond the depositional area of turbiditic sand and silt, which may explain why the turbiditic mudstone beds – instead of capping turbidites – often overlie debrites or the other mudstone varieties of facies F4. The lamination in mudstone is probably not tractional and can be due to the rhythmic depletion of a stable density gradient of quasi-standing suspension cloud by sedimentation-driven convection (Kerr 1991). Some of the massive, non-laminated mudstone beds may represent spontaneous gravity flows of fluidal mud (Baas *et al.* 2009) unrelated directly to turbidity currents.

Facies F5: Marlstone

Description: This facies comprises isolated beds of marlstone, bluish white (locally greenish or grey to reddish) in colour, with thickness up to 30 cm, but rarely more than 5 cm (Text-figs 4B–D and 5A). The lower bed boundaries are mainly sharp, but rarely erosional, whereas the upper boundaries range from sharp (in cases of an overlying sandstone) to gradational (in cases of an overlying mudstone). The majority of marlstone beds are massive, non-laminated, and show macroscopic normal grading only where containing an admixture of sand and silt. Non-
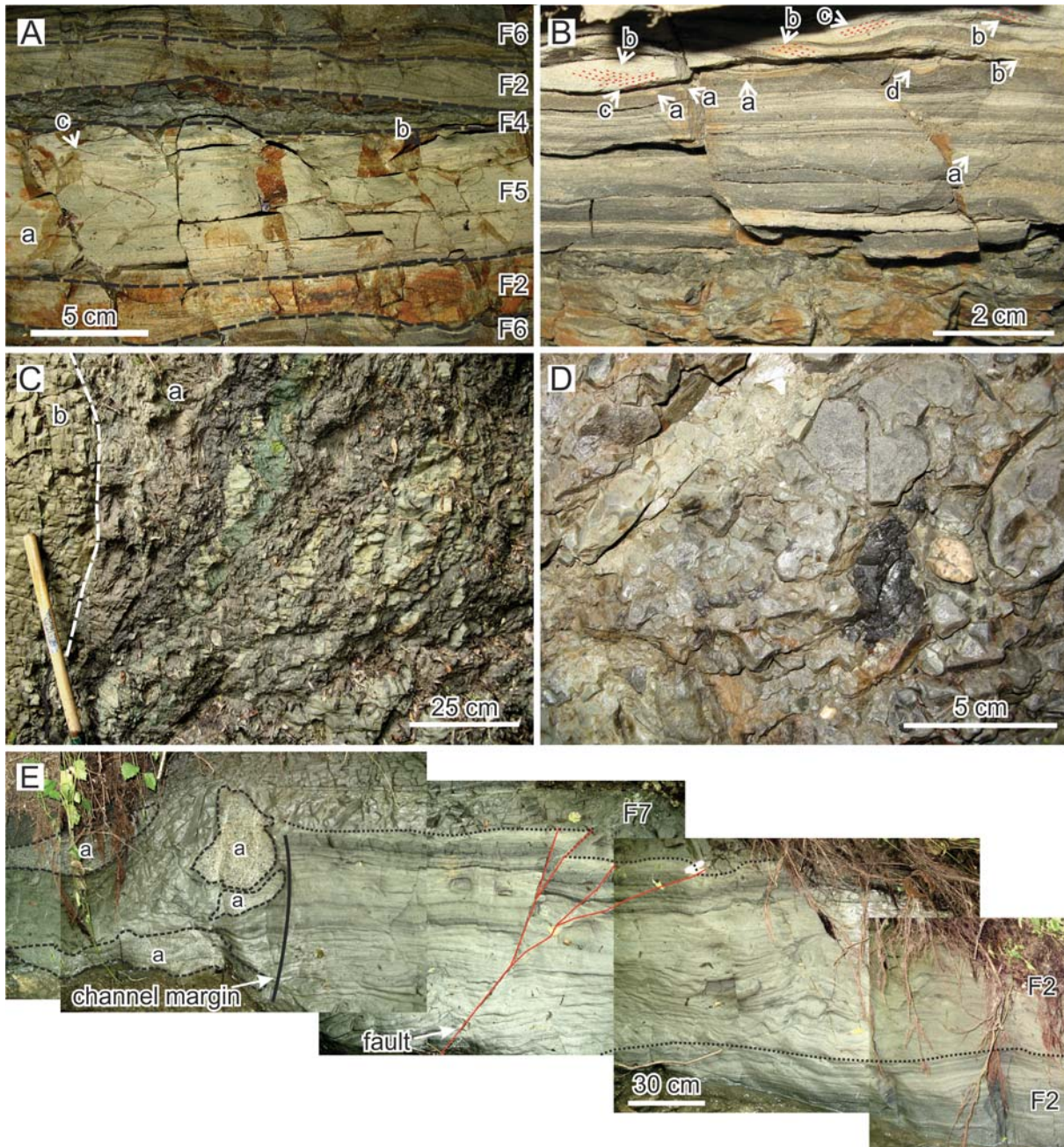
Text-fig. 5. Outcrop examples of facies F5, F6 and F7; A – Marlstone bed of facies F5 with sandy laminae (a), starved ripples (b) and starved ripples with marlstone drapes (c); note the underlying layers of facies F2 and F6 and the overlying layers of facies F4, F2 and F6; B – Heterolithic deposit of facies F6 composed of mud with planar laminae of silt and very fine-grained sand, showing burrows (a) and starved ripples with palaeotransport direction both to the right (b) and to the left (c); some ripples are loaded (d); C – Mud-rich debrite of facies F7 (a), with scattered intraformational clasts of sand, silt and mud, underlain by sandstone of facies F1 (b); beds are subvertical; D – Mud-rich debrite of facies F7 with scattered intraformational and exotic clasts; E – Outcrop photomosaic of a faulted palaeochannel margin in parallel-stratified sandstone of facies F2, buried by a debrite of facies F7 with large intraformational balls of facies F2 sandstone and facies F1 conglomerate (a)

bioturbated beds show parallel lamination or wispy lamination related to silt admixture. The thicker beds contain interlayers of quartzose very fine sandstone or siltstone, around 1 cm thick, with planar parallel lamination, ripple cross-lamination and marl-draped starved-ripple lenses (Text-fig. 5A).

Marlstone beds show abundant bioturbation structures, with burrows invariably filled with dark mud, even where such sediment is not present directly above or below the marlstone. Common are *Chondrites* isp., *Planolites* isp., *Scolicia* isp. and *Ophiomorpha* isp. Biogenic micrite consists mostly of planktic foraminifer tests, fragments of carbonate sponge spicules and shell detritus. Non-calcareous component is a variable admixture of quartz grains, coalified plant detritus, pyrite, muscovite flakes and glauconite grains. Facies F5 is difficult to distinguish from facies F4 in some poorer exposed or less accessible parts of the outcrop section, as these rocks are often similar in colour and mudstone is variably calcareous.

Interpretation: Based on the evidence of normal grading, lamination and relatively high admixture of non-calcareous sediment, the beds of facies F5 are interpreted as deposits of highly dilute, muddy calciturbiditic currents (cf. Stow and Bowen 1978, 1980). The deposits would be genetically comparably to the Bouma (1962) turbidites $T_{(B)CDE}$, but characterized by sparse sandy or silty tractional lower divisions and dominant post-tractional fallout divisions. The paucity of visible lamination is due to bioturbation, as the less bioturbated beds seem to show traces of faint parallel lamination almost throughout to the top. The lamination in marly turbidite divisions DE is unlikely to be tractional and can be due to the rhythmic depletion of a stable density gradient of quasi-standing suspension cloud by sedimentation-driven convection (Kerr 1991), whereas some of the non-laminated marlstone beds may be unrelated to turbidity currents and represent spontaneous gravity flows of fluidal mud (Baas *et al.* 2009).

Beds with multiple normal grading (Text-fig. 5A) may represent successive flows following closely one another as pulses or may reflect flow internal pulses driven by interface Kelvin-Helmholtz waves (cf. Ge *et al.* 2017). However, it cannot be precluded that the internal sandy/silty tractional divisions within a marlstone bed were inserted by the independent action of tidal or contouritic bottom currents (cf. Shanmugam 2008, 2017; Stow and Faugères 2008; Dykstra 2012).

The intense bioturbation of marlstones implies well-oxygenated seafloor conditions with an adequate supply of nutrients for benthic organisms to thrive. The mudstone facies F4, in contrast, signifies relatively dysoxic and oligotrophic conditions.

Facies F6: Heterolithic deposits

Description: Facies F6 occurs as units, up to 47 cm thick, of white, yellowish white or grey calcareous siltstone and very fine-grained sandstone intercalated with mudstone (Text-fig. 5B). Most such units are only several centimetres thick, with an uneven pinch-and-swell geometry. The thin heterolithic bedding is well pronounced, as the boundaries of the sandstone or siltstone layers and the mudstone layers are sharp, locally loaded (Text-fig. 5B), with flame structures, flute marks and bioturbation features. The sandstone and siltstone beds show internal plane-parallel lamination and climbing or non-climbing ripple cross-lamination, commonly with mud drapes or flasers, but beds are laterally discontinuous, comprised of starved and/or loaded ripple lenses. The successive ripple cross-laminae sets occasionally show significantly different or opposite palaeoflow directions (Text-fig. 5B). Recognizable trace fossils are *Ophiomorpha* isp*., Scolicia* isp. and *Planolites* isp., occurring as endichnia and hypichnia (Text-fig. 5B). Some beds are virtually homogenized by intense bioturbation. Mudstone is similar as in facies F4 and some of its layers contain parallel or wispy laminae of silty and fine sand, which makes the distinction locally difficult and somewhat arbitrary – based on the facies context.

Interpretation: Facies F6 indicates an action of short-lived or markedly pulsating, discrete tractional currents alternating with episodes of 'background' mud suspension fallout. Such depositional conditions may represent: (i) episodic incursions of the dilute tails of turbidity currents into an area of hemipelagic mud deposition; (ii) episodic spill-out of channelized turbidity currents into such an area; or (iii) episodic action of fluctuating contour currents or tidal currents (cf. He *et al.* 2008; Shanmugam 2008, 2017; Dykstra 2012). An involvement of tidal currents seems to be supported by the sharp but non-erosional bed boundaries, mud flasers in ripple cross-laminae sets and occasional evidence of palaeocurrent reversals.

Facies F7: Massive mud-rich conglomerate and pebbly or sandy

Description: This facies includes isolated and relatively thick, non-graded massive beds of mud-rich conglomerates and pebbly or sandy mudstones (Text-figs 4E, 5C–E). Conglomerate beds are a few decimetres to more than 600 cm thick, matrix-supported and containing intraformational and/or exotic clasts. Matrix is a mud-rich sand. Bed bases are sharp and often deformed by loading, but not necessarily erosional. Intraformational debris includes cobble- to boulder-sized fragments of mudstone, marlstone and siltstone (Text-fig. 5C), glauconite-rich sandstone,

as well as ball-shaped fragments of fine- to coarse-grained sandstone and granule conglomerate (Text-fig. 5E). The intraclasts are mainly subrounded and their lithological range corresponds to the associated other sedimentary facies. Some sandstone boulders are up to 40 x 100 cm in size, whereas mudstone boulders are plastically deformed and partly disintegrated, merged with the muddy matrix. Smaller clasts tend to be deformed into lenses oriented mainly parallel to bedding (Text-fig. 5C). Clasts of marlstone and mudstone are often armoured with coarse sand and granules. The intraformational conglomerate beds occur in segments E–G of the stratigraphic section (Text-fig. 3).

Conglomerate beds with exotic clasts occur only in the section's segments H and I (Text-fig. 3). They are similarly mud-rich and matrix-supported, 40 cm and to more than 350 cm in thickness, usually capped by sandstone facies F2. The bed bases are mainly flat, with no evidence of significant erosion or deformation. In addition to intraformational debris (comparable lithologically to facies F1, F2 and F3), these beds contain scattered, rounded pebble-sized exotic clasts of a Štramberk-type limestone (cf. Hoffmann et al. 2017), greenschist, coal, igneous and volcanic rocks, and subordinately some other sedimentary and metamorphic rocks (Text-fig. 5D). The volumetric ratio of clast to matrix is lower than in the purely intraformational conglomerates. The lithological composition of exotic clasts is similar to that reported from the conglomerates and pebbly mudstones in the Upper Cretaceous of the Silesian Nappe (Strzeboński et al. 2017) and from the Ropianka Formation elsewhere in the Skole Nappe (Łapcik et al. 2016).

The third variety of facies F7 deposits are isolated massive beds of pebbly or sandy mudstone (Text-fig. 4E), several decimetres to more than 500 cm in thickness. They are similarly non-graded, containing randomly scattered, sparse quartz pebbles and small intraclasts lithologically similar to facies F4, F5 and F6. In contrast to facies F4 and F5, the mudstones of facies F7 show little or no bioturbation. These deposits occur only in segment I of the stratigraphic section (Text-fig. 3), where they alternate with thick-bedded muddy sandstones of facies F3.

Interpretation: The deposits of facies F7 are interpreted to be debrites emplaced as highly cohesive debris flows and mudflows (cf. Crowell 1957; Prior et al. 1984; Mulder and Alexander 2001; Shanmugham 2006, 2016b; Talling et al. 2012; Strzeboński et al. 2017). The intraformational conglomerates, with plastically deformed sedimentary slabs and disrupted ball-and-pillow features, represent various stages of a

mass-movement transformation from slump into debris flow. The preservation of intraformational clasts, which were originally soft, suggests relatively short mass-flow distances, or perhaps some longer-runout slow-moving or hydroplaned fast-moving flows with limited internal shear. The hydroplaning of mud-rich debris flows and mudflows (e.g., Mohrig et al. 1998; Gee et al. 1999; Ilstad et al. 2004) is particularly invoked to explain their non-erosive long runout with little or no internal shearing. The same emplacement mechanisms of slow or hydroplaned fast movement may apply to the sandy mudstones and muddy conglomerates with exotic gravel, which signify a markedly heterolithic source with sediment mixing during its gravitational collapse. The common occurrence of sandstone facies F2 with exotic gravel at the top of pebbly mudstone bed may indicate a turbiditic current triggered by retrogressive failure directly after the initial slumping and debris flow. Some of the gravel-free mudstones and sandy mudstones may be the so-called 'unifites' (e.g., Stow and Bowen 1978, 1980; Ricci Lucchi and Valmori 1980; McCave and Jones 1988; Talling et al. 2012), and their thickest beds may be due to amalgamation of two or more consecutive flows.

Muddy debrites comparable to facies F7 are common in basin-slope settings, and are known to occur in within the slope, at the base of slope and in more distal basin-floor areas (e.g., Gee et al. 1999; Tripsanas et al. 2008; Shanmugam 2016b). The deposits of facies F7 may then represent cohesive debris flows derived locally from the basin's adjoining northern slope or generated within the base-of-slope system by the collapses of channel cut-banks and levees. The textural variation of deposits suggests that a combination of these sources is likely. The sediment gravity movements may have been spontaneous or triggered by earthquakes, or both.

FACIES ASSOCIATIONS

Based on the stratigraphic grouping of sedimentary facies and their upward grain-size trends (Text-fig. 3), six facies associations have been distinguished – differing in their facies composition, the mean value, median and variance of bed thicknesses and the sandstone net/gross percentage (see data summary in Table 1). On the account of their component facies characteristics (depositional processes), the individual facies associations are interpreted as representing different morphodynamic sub-environments of the submarine depositional system. The

Channel-fill facies association			Channel-mouth lobe facies association		
Package thickness: 3.8–21.1 m (mean 12.7 m)			Package thickness: 2–8 m (mean 5.7 m)		
Component facies thickness contribution:	Individual facies bed thicknesses:		Component facies thickness contribution:	Individual facies bed thicknesses:	
F1	36.7 %	4–195 cm (mean 53.6 cm)	F2	43.1 %	1–120 cm (mean 14.8 cm)
F2	26.6 %	3–118 cm (mean 24.1 cm)	F1	22.4 %	12–59 cm (mean 32.6 cm)
F3	15.5 %	6–150 cm (mean 61.8 cm)	F4	12.9 %	1–24 cm (mean 3.8 cm)
F7	7.2 %	22–219 cm (mean 108.5 cm)	F3	9.6 %	18–50 cm (mean 26.4 cm)
F4	6.2 %	1–18 cm (mean 4.4 cm)	F5	6.3 %	1–12 cm (mean 4.7 cm)
F6	5 %	1–30 cm (mean 6.6 cm)	F6	5.7 %	1–25 cm (mean 6.2 cm)
F5	2.8 %	1–15 cm (mean 4.9 cm)			
Sandstone bed thicknesses: Median = 27 cm Mean = 38.7 cm Variance = 1408 cm^2 Standard deviation = 37.5 cm Sandstone net/gross = 61.5–93.6 % (mean 78.1 %)			Sandstone bed thicknesses: Median = 12 cm Mean = 19.3 cm Variance = 335.1 cm^2 Standard deviation = 18.3 cm Sandstone net/gross = 61.8–97.9 % (mean 81.7 %)		
Channel-levee facies association			**Interlobe basin-plain facies association**		
Package thickness: 3.8–6.1 m (mean 4.6 m)			Package thickness: 0.05–5.1 m (mean 1.4 m)		
Component facies thickness contribution:	Individual facies bed thicknesses:		Component facies thickness contribution:	Individual facies bed thicknesses:	
F2	40 %	1–41 cm (mean 7.4 cm)	F2	41.2 %	1–19 cm (mean 6 cm)
F5	21.8 %	1–15 cm (mean 5.6 cm)	F5	23.8 %	1–16 cm (mean 4.8 cm)
F1	19.9 %	16–52 cm (mean 31 cm)	F4	22 %	1–14 cm (mean 2.6 cm)
F4	13.9 %	1–15 cm (mean 2.7 cm)	F6	13 %	1–30 cm (mean 6.5 cm)
F6	4.4 %	1–20 cm (mean 4.1 cm)			
Sandstone bed thicknesses: Median = 6 cm Mean = 9.9 cm Variance = 102.8 cm^2 Standard deviation = 10.1 cm Sandstone net/gross = 44–67.5% (mean 58.9 %)			Sandstone bed thicknesses: Median = 5 cm Mean = 5.3 cm Variance = 11.2 cm^2 Standard deviation = 3.3 cm Sandstone net/gross = 0–63.2 % (mean 41 %)		
Crevasse-fill facies association			**Crevasse-splay facies association**		
Package thickness: 4.8 m			Package thickness: 0.08–0.78 m (mean 0.32 m)		
Component facies thickness contribution:	Individual facies bed thicknesses:		Component facies thickness contribution:	Individual facies bed thicknesses:	
F1	35 %	11–50 cm (mean 28 cm)	F1	63.7 %	7–45 cm (mean 20.3 cm)
F2	34.4 %	2–18 cm (mean 7.2 cm)	F2	27 %	2–25 cm (mean 7.4 cm)
F4	17.1 %	1–13 cm (mean 2.8 cm)	F3	9.3 %	14–38 cm (mean 24.7 cm)
F5	10.8 %	1–10 cm (mean 5.2 cm)			
F6	2.7 %	1–4 cm (mean 2.2 cm)			
Sandstone bed thicknesses: Median = 6 cm Mean = 11.5 cm Variance = 122.7 cm^2 Standard deviation = 11.1 cm Sandstone net/gross = 69.4 %			Sandstone bed thicknesses: Median = 12 cm Mean = 14.5 cm Variance = 123.4 cm^2 Standard deviation = 11.6 cm Sandstone net/gross = 100 %		

Table 1. Quantitative summary of the characteristics of facies associations in the Hucisko Jawornickie section

vertical organization of facies within their particular associations, or the time pattern of the operation of depositional processes within a particular sub-environment, has been analysed with the use of the stochastic method of embedded Markov chains (for description, see Davis 2002).

Channel-fill facies association

Description: The facies assemblages of this type are 3.8–21.1 m thick (mean ca. 13 m), have a sandstone net/gross of 62% to 94% and are dominated by facies F1 (37%), F2 (27%) and F3 (16%), with only minor contribution of the finer-grained facies F4, F5, F6 and F7 (Table 1). Facies F1, F2, F3 and F7 reach here their greatest bed thicknesses in this facies assemblage, and the overall variance of bed thicknesses is the highest, with a standard deviation (SD) of 37.5 cm. The mean sandstone bed thickness ($M = 39$ cm) is higher than the median ($Md = 27$ cm), which indicates a positively skewed bed-thickness frequency distribution, with an excess of thicker beds. These

Channel-fill facies association

Transition count matrix

	F1	F2	F3	F4	F5	F6	F7
F1		4	2	19	5	6	2
F2	8		3	30	13	7	1
F3	2	5		7	1	1	1
F4	16	29	9		6	21	0
F5	4	13	1	7		9	0
F6	6	7	0	21	9		0
F7	0	4	0	0	0	0	

Difference matrix

	F1	F2	F3	F4	F5	F6	F7
F1		-0.15	-0.02	0.16	-0.01	-0.02	0.04
F2	-0.05		-0.03	0.11	0.05	-0.09	0
F3	-0.03	0.06		0.10	-0.07	-0.11	0.04
F4	0.01	0.04	0.03		-0.10	0.04	-0.02
F5	-0.04	0.13	-0.04	-0.12		0.09	-0.02
F6	-0.02	-0.10	-0.07	0.15	0.07		-0.02
F7	-0.14	0.77	-0.06	-0.29	-0.12	-0.16	

F6 ⇄ F5 ⇄ F2 ⇄ F4 ⇄ F1   F3 ➝ F7
(marl)
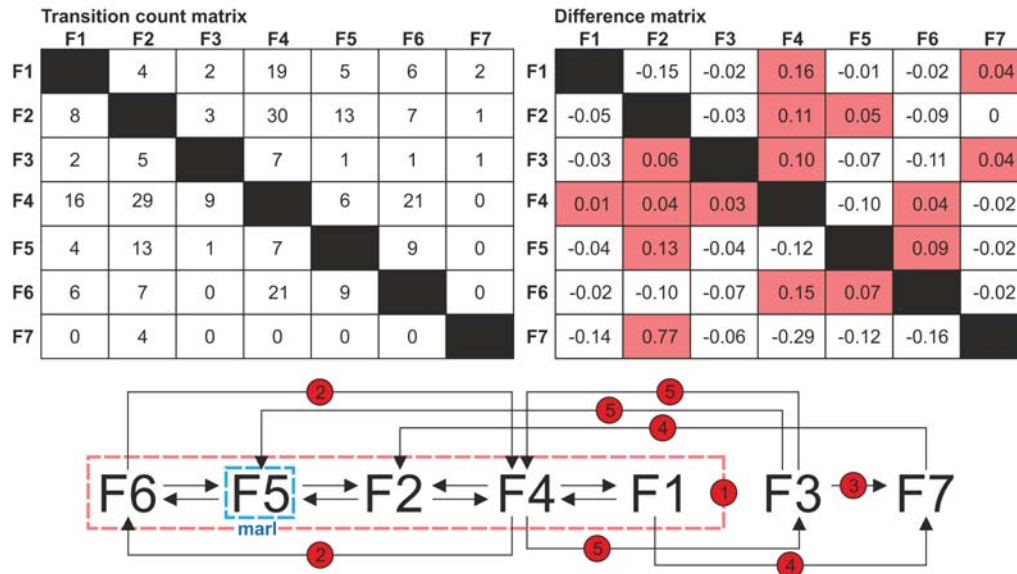
① Succession of alternating facies F1-F4-F2-F5-F6 with a general fining- and thinning-upwards trend.

② Episodes of intra-channel stagnation (F4) alternate with heterolithic sedimentation involving weak/small tractional currents (F6).

③ Emplacement of sandy debris flow (F3) followed by mud-rich cohesive debris flow (F7), perhaps due to stepwise bank collapse.

④ Erosive passage of 1–2 high-density turbidity currents (F1) triggers cohesive slump/debris flow (F7), followed by 1–2 low-density turbidity currents (F2).

⑤ Episode of intra-channel stagnation (F4) is interrupted by emplacement of sandy debris flow (F3), followed by further stagnation (F4) or deposition of marl with weak/small tractional currents (F5).

Text-fig. 6. Transition-count and difference matrices for channel-fill facies association with the corresponding Markov chain model of facies vertical organization and an interpretation of particular facies transitions. The total number of counted facies transitions is $N = 279$ and the confidence level of difference matrix is 99%. The preferential facies transitions (more frequent than random) are highlighted in colour in the difference matrix and are the basis of Markov chain model

facies assemblages show a non-systematic thinning- and fining-upwards trend, perturbed by the irregular insertion of debrite facies. The preferential pattern of upwards facies transition in this type of facies assemblages is shown as a Markov chain model in Text-fig. 6.
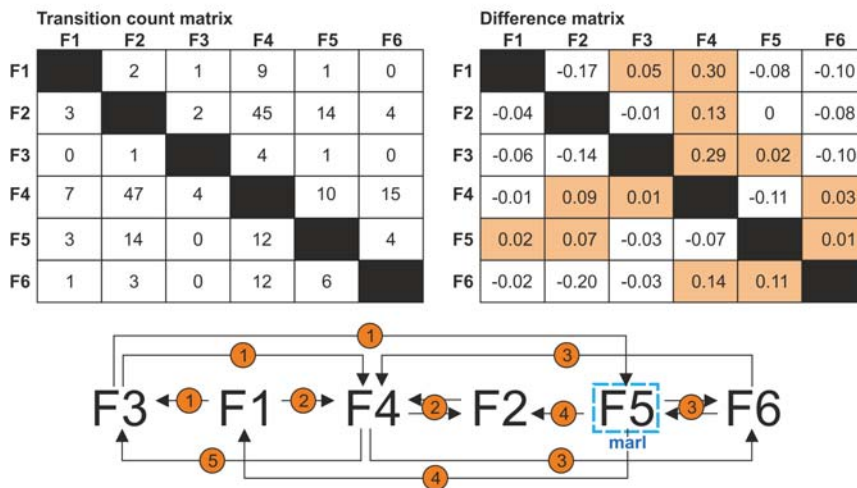
Interpretation: These facies assemblages – as the richest in sandstone and conglomeratic facies, with the highest amount of erosional bed amalgamation and a finning- and thinning-upwards trend – is interpreted as the infill of distributary channels (cf. Mutti and Normark 1987; Pickering *et al.* 1995; Clark and Pickering 1996; Bruhn and Walker 1997; Stow and Mayall 2000; Gardner *et al.* 2003; Mayall *et al.* 2006; Posamentier and Walker 2006; Janbu *et al.* 2007; Hubbard *et al.* 2008, 2014; Bernhardt *et al.* 2011; McHargue *et al.* 2011; Mulder 2011; Janocko *et al.*

2013; Bayliss and Pickering 2015a, b; Pickering *et al.* 2015; Shanmugam 2016a; Łapcik 2018). Submarine channels around 20 m deep would likely be only a few hundred metres wide (Clark and Pickering 1996), which supports the notion of cut-and-fill avulsive distributaries, rather than the system's longer-lived main feeder conduits. The channel-fill sedimentation dynamics, in terms of the modal upward trend of depositional processes, is interpreted in detail in Text-fig. 6.

Channel-mouth lobe facies association

Description: Facies assemblages of this type are 2–8 m thick, have a sandstone net/gross of 62% to 98% and are dominated by sandstone facies F1, F2 and F3 (jointly 75%), while lacking facies F7 (Table
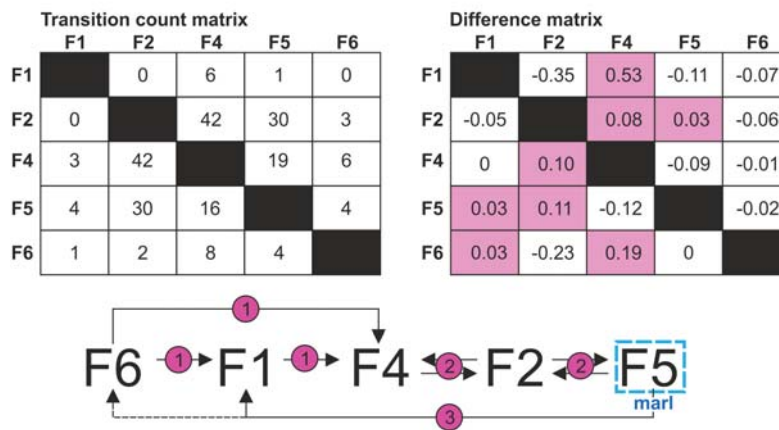
Text-fig. 7. Transition-count and difference matrices for channel-mouth lobe facies association with the corresponding Markov chain model of facies vertical organization and an interpretation of particular facies transitions. The total number of counted facies transitions is $N = 225$ and the confidence level of difference matrix is 80%. The preferential facies transitions (more frequent than random) are highlighted in colour in the difference matrix and are the basis of Markov chain model

1). Compared to the channel-fill facies association, the mean contribution of facies F2 here is higher (43%) and the contribution of facies F1 (22%) and facies F3 (10%) is lower. Significantly higher is the contribution of fine-grained facies F4 (13%) and facies F5 (6%). The sandstone beds of facies F1, F2 and F3 are much thinner and show a considerably lower thickness variance, with a standard deviation of 18 cm (Table 1). Also here, the mean sandstone bed thickness ($M = 19$ cm) is higher than the median ($Md = 12$ cm), which indicates a slightly positive skewness of the bed-thickness frequency distribution and hence an excess of thicker beds. These facies assemblages tend to show a non-systematic coarsening- and thickening-upwards trend. Their modal pattern of upward facies organization is shown as a Markov chain model in Text-fig. 7.

Interpretation: This type of facies assemblages is the second richest in sandstones, but in comparison to the previous one, it is finer-grained and thinner bedded, dominated by the tabular sandstone beds of facies F2, with much less amalgamation of beds and a higher contribution of the intervening fine-grained facies. The sandstone net/gross and bed-thickness statistics seem to reflect those of the channel-fill facies association (Table 1). This second type of facies association is thus considered to be a distal equivalent of the previous one and represent channel-mouth depositional lobes (cf. Mutti and Normark 1987; Shanmugam and Moiola 1991; Pickering *et al.* 1995; Stow and Mayall 2000; Deptuck *et al.* 2008; Prélat *et al.* 2009; Bernhardt *et al.* 2011; Mulder 2011; Grundvåg *et al.* 2014; Marini *et al.* 2015; Shanmugam 2016a; Łapcik 2017). The notion of depositional lobes is supported by the sparsity of bed erosional amalgamation and the coarsening- and thickening-upwards trend. The sedimentation dynamics of channel-mouth lobe accretion, in terms of the modal upward pattern of depositional processes, is interpreted in detail in Text-fig. 7.

Text-fig. 8. Transition-count and difference matrices for channel-levee facies association with the corresponding Markov chain model of facies vertical organization and an interpretation of particular facies transitions. The total number of counted facies transitions is $N = 221$ and the confidence level of difference matrix is 97.5%. The preferential facies transitions (more frequent than random) are highlighted in colour in the difference matrix and are the basis of Markov chain model
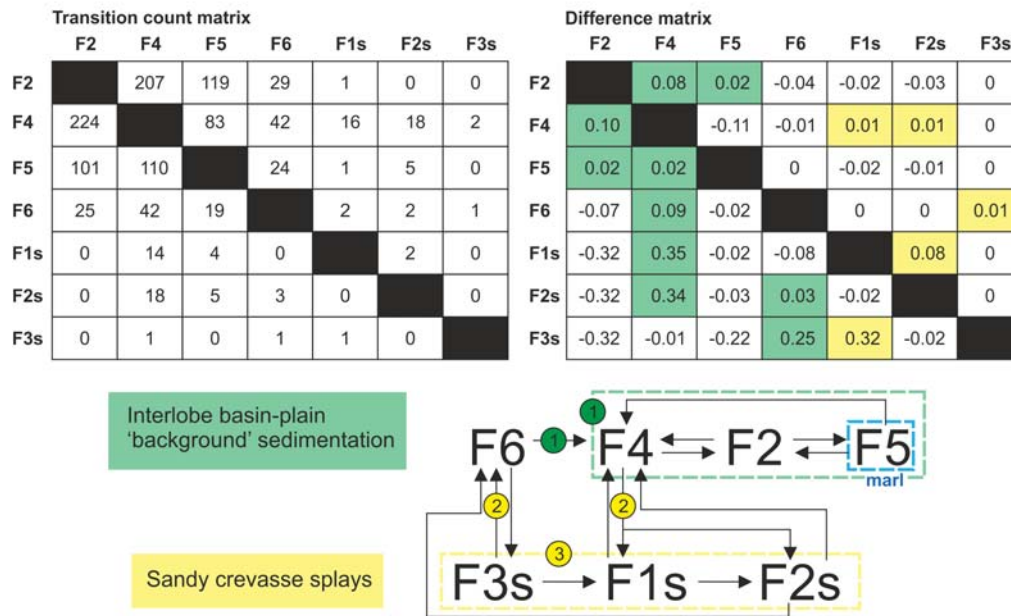
Channel-levee facies association

Description: This third type of facies assemblages is 3.8–6.1 m thick (mean 4.6 m), has a sandstone net/gross of 44% to 68% and is dominated by thin-bedded sandstone facies F2 (40%) and F1 (20%), but lacking facies F3 and F7 (Table 1). The thickness contribution of fine-grained facies is similar as in the previous facies association, but the relative proportion of marlstone facies F5 (22%) is higher. Despite the apparent similarity to the previous facies association, the mean thickness of sandstone beds ($M = 10$ cm) and their median ($Md = 6$ cm) are nearly half-lower, and particularly the beds of facies F2, F4 and F6 are by comparison much thinner (Table 1). Furthermore, the bulk variance of sandstone bed thicknesses is much lower, with a standard deviation of only 10 cm. These facies assemblages show a non-systematic and often multiple coarsening- and thickening-upwards trend. Their bulk modal pattern of vertical facies organization is shown as a Markov chain model in Text-fig. 8.

Interpretation: The sedimentary characteristics of this type of facies assemblages suggest that they are like thinner-bedded imitations of the previous facies association, but with a lower sandstone net/gross, a higher proportion of marlstone facies F5 and a lack of facies F3 and F7. These facies assemblages are interpreted as levee deposits of distributary channels, a notion supported by their coarsening- and thickening-upwards trend and their direct association with inferred crevasse-fill and interlobe overbank deposits (described further below). Deposition of levees up to at least 6 m thick may indicate sinuous channels or local channel bends, where flow spill-out would be enhanced (cf. Pickering *et al.* 1995; Clark and Pickering 1996; Bruhn and Walker 1997; Posamentier and Walker 2006; Hubbard *et al.* 2008; Mulder 2011; Janocko *et al.* 2013; Bayliss and Pickering 2015a, b). The slight positive skewness of the sandstone bed-thickness frequency distribution ($M > Md$) indicates an excess of thicker beds and seems to reflect the sedimentation dynamics of channel-fill and lobe deposition. The modal pattern of depositional processes represented by facies organization is interpreted in detail in Text-fig. 8.

Interlobe basin-plain & crevasse-splay facies associations

Text-fig. 9. Transition-count and difference matrices for interlobe basin-plain and crevasse-splay facies associations with the corresponding joint Markov chain model of facies vertical organization and an interpretation of particular facies transitions. The total number of counted facies transitions is $N = 1122$ and the confidence level of difference matrix is 99.9%. The preferential facies transitions (more frequent than random) are highlighted in colour in the difference matrix and are the basis of Markov chain model

Interlobe basin-plain and crevasse-splay facies associations

Description: This fourth type of facies assemblage occurs as stratigraphic intervals several tens of metres thick in the outcrop section's segments A and B (Text-fig. 3). It consists of the fine-grained packages of thinly bedded facies F2, F4, F5 and F6 intercalated with 'outsized' sandstone beds composed of facies F1, F2 and F3. The fine-grained packages are up to 5.1 m thick (mean 1.4 m), have a sandstone net/gross of 0% to 63% (mean 41%), and lack such component facies as F1, F3 and F7 (see interlobe association in Table 1). Thin-bedded sandstone facies

F2 abounds (41%), the contribution of fine-grained facies F4 (22%) and F6 (13%) is higher than in the other facies assemblages, and the contribution of facies F5 (24%) is the highest in the entire succession. The beds here are thinnest, with a mean thickness ($M = 5$ cm) equal to median ($Md = 5$ cm) and a low standard deviation of 3 cm. The intervening outsized sandstone beds consist of a combination of facies F1, F2 and F3 (for details, see crevasse-splay association in Table 1). The modal upward facies organization of these associations is shown as a joint Markov chain model in Text-fig. 9 (with the facies components of outsized sandstone beds labelled with suffix 's').

*Interpretation:* This thinnest-bedded and fin-

est-grained facies association occurs between the sand-dominated channel-lobe assemblages and is interpreted as interlobe basin-plain deposits, variously interspersed with crevasse-splay sandstone sheets. The occurrence of crevasse splays supports the notion of interlobe areas evacuated by the lateral switching of depositional lobes, rather than distal areas of lobe 'feather-edge' termini (cf. Pickering *et al.* 1995; Deptuck *et al.* 2008; Prélat *et al.* 2009; Grundvåg *et al.* 2014; Łapcik 2017). The modal pattern of depositional processes represented by vertical facies organization is interpreted in detail in Text-fig. 9.

Crevasse-fill facies association

Description: This subordinate facies assemblage occurs only once in segment B of the outcrop section (Text-fig. 3), where it is 4.8 m thick and shows a sandstone net/gross of nearly 70%. It is dominated in equal proportion by sandstone facies F1 (35%) and F2 (34%), with some contribution of fine-grained facies F4 (17%), F5 (11%) and F6 (3%), and has a fining- and thinning-upwards trend. Facies F3 and F7 are lacking (Table 1). Beds thicknesses are comparable to those

in the channel-levee assemblages, but their variance and standard deviation are slightly higher and the mean thickness of facies F6 beds is half-lower (2 cm). The mean thickness of sandstone beds ($M = 11.5$ cm) is higher than the median ($Md = 6$ cm), which indicates an excess of thicker beds – as in the channel-fill and channel-related facies assemblages (Table 1). In contrast to the channel-levee assemblages, this assemblage has an erosional base and shows an irregular fining- and thinning-upwards trend. Its modal upward facies organization is summarized as a Markov chain model in Text-fig. 10.

Interpretation: This facies assemblage resembles to some extent the channel-levee assemblages, but is markedly richer in sandstones. Its erosional base, discernible fining- and thinning-upwards trend and direct association with channel-levee deposits suggest that this facies assemblage is a crevasse-fill – the infill of a spill-out channel cut across distributary channel levee (Carter, 1988; Klaucke and Hesse 1996; Nakajima *et al.* 1998). The modal pattern of depositional processes recognized from vertical facies organization is interpreted in detail in Text-fig. 10. The notion of crevasses in the sedimentary system is
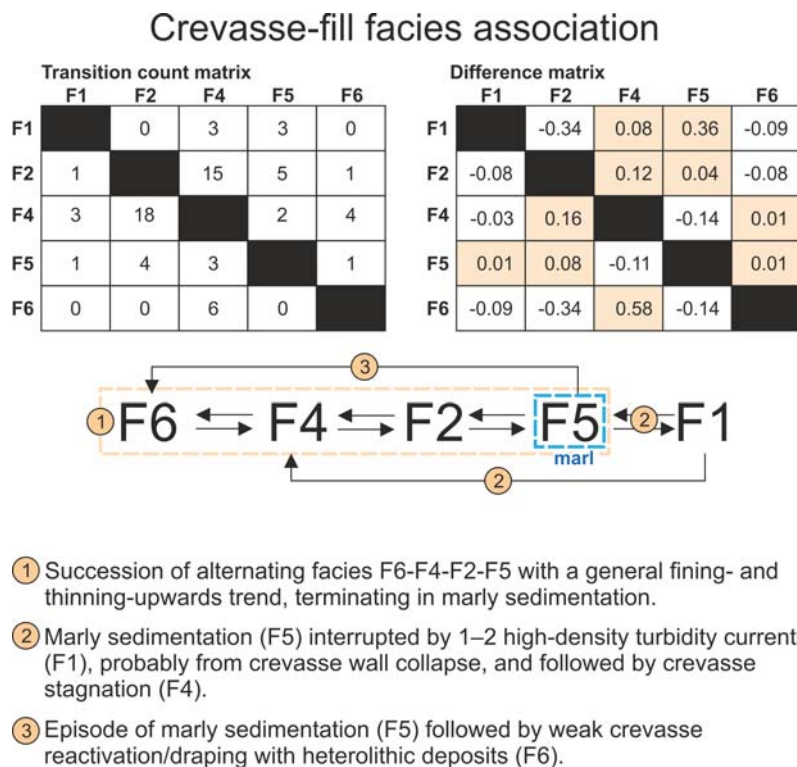
Text-fig. 10. Transition-count and difference matrices for crevasse-fill facies association with the corresponding Markov chain model of facies vertical organization and an interpretation of particular facies transitions. The total number of counted facies transitions is $N = 70$ and the confidence level of difference matrix is 90%. The preferential facies transitions (more frequent than random) are highlighted in colour in the difference matrix and are the basis of Markov chain model

consistent with the inferred crevasse-splay deposits (Table 1). Crevasses indicate channel propensity for avulsion and their sporadic preservation is simply a record of failed avulsion attempts.

DEPOSITIONAL MODEL

Based on the six facies associations recognized in the Hucisko Jawornickie section (Table 1), the sedimentary palaeosystem studied is envisaged as a progradational base-of-slope complex of depositional lobes fed by avulsive sinuous channels with levees, crevasses and numerous crevasse splays (Text-fig. 11A). The channel-mouth lobes and channel-fill bodies would be lenticular in transverse cross-section and hence it is reasonable to assume that only their maximum thicknesses measured in a single longitudinal outcrop section may be representative when it comes to the system dimensions. These maximum thickness are in the lowest range of values for similar features reported from elsewhere by other authors (e.g., Gardner *et al.* 2003; Mayall *et al.* 2006; Posamentier and Walker 2006; Janbu *et al.* 2007; Deptuck *et al.* 2008; Prélat *et al.* 2009; Bernhardt *et al.* 2011; McHargue *et al.* 2011; Mulder 2011; Janocko *et al.* 2013; Hubbard *et al.* 2014; Grundvåg *et al.* 2014; Bayliss and Pickering 2015a; Marini *et al.* 2015; Pickering *et al.* 2015; Shamugam 2016a). The maximum thickness of channel-fill bodies (21.1 m, Table 1), with a 20% correction for sediment compaction, would suggest distributary channels up to 21.5 m deep. The statistically expected width of such channels would be in the range of 100 m to 1000 m (Clark and Pickering 1996; Clark and Gardiner 2000). Assuming a moderate channel width of 0.5 km and a levee width around 1 km, the width of a channel-and-levee complex would be around 2.5 km, which suggests a radial length of depositional lobe around 3.5 km (Howell and Normark 1982). This estimate is similar to that made independently by Łapcik (2017) from another outcrop section of the Ropianka Formation, pointing to a relatively small size of turbiditic channels and depositional lobes in the Skole Basin (cf. global data in Howell and Normark 1982; Clark and Pickering 1996; Clark and Gardiner 2000).

The measured cumulative thickness of the sedimentary succession is more than 400 m, which means that – in addition to the build-out of depositional lobes and downstream extension of their distributary channels – the lobe complex was strongly aggrading. Therefore, a crucial component of the system morphodynamics was the lateral avulsive shifting of

Facies associations:

- Channel-fill deposits
- Channel-levee deposits
- Crevasse-fill deposits
- Channel-mouth lobe deposits
- Crevasse-splay deposits
- Interlobe basin-plain deposits

Lobe-complex dynamics
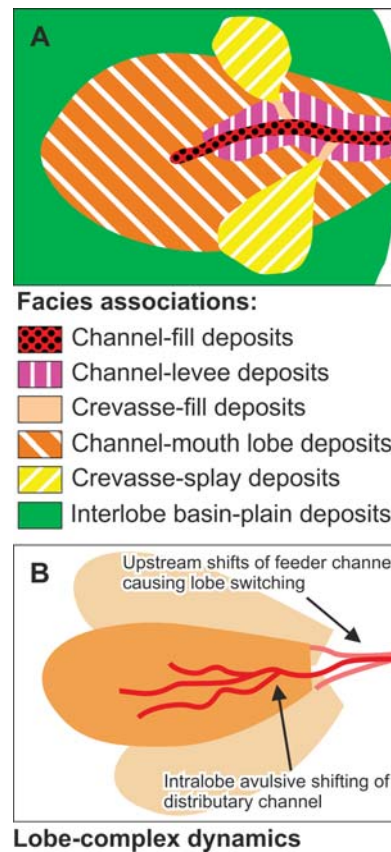
Text-fig. 11. Schematic dimensionless conceptual model for the depositional palaeosystem studied in the Hucisko Jawornickie section (for hypothetical dimensional estimates, see text); A – Spatial relationships of the depositional sub-environments (facies associations) in the system; B – The key morphodynamic factors postulated for the stratigraphic development of an aggrading system

distributary channel within a lobe area and the lateral switching of depositional lobes due to upstream shifts of main feeder channel (Text-fig. 11B). This morphodynamic scenario is consistent with widely held concepts (e.g., Normark *et al.* 1993; Ferry *et al.* 2005; Deptuck *et al.* 2007; Cantelli *et al.* 2011; Hodgson *et al.* 2011; Hubbard *et al.* 2014) and serves to explain the stratigraphic architecture of facies assemblages stacked vertically in the sedimentary succession, as discussed in the next section.

DYNAMIC STRATIGRAPHY

The sedimentary succession in the Hucisko Jawornickie outcrop section (Text-fig. 3) is interpreted as a base-of-slope channelized lobe complex that prograded basinwards over the distal, non-chan-
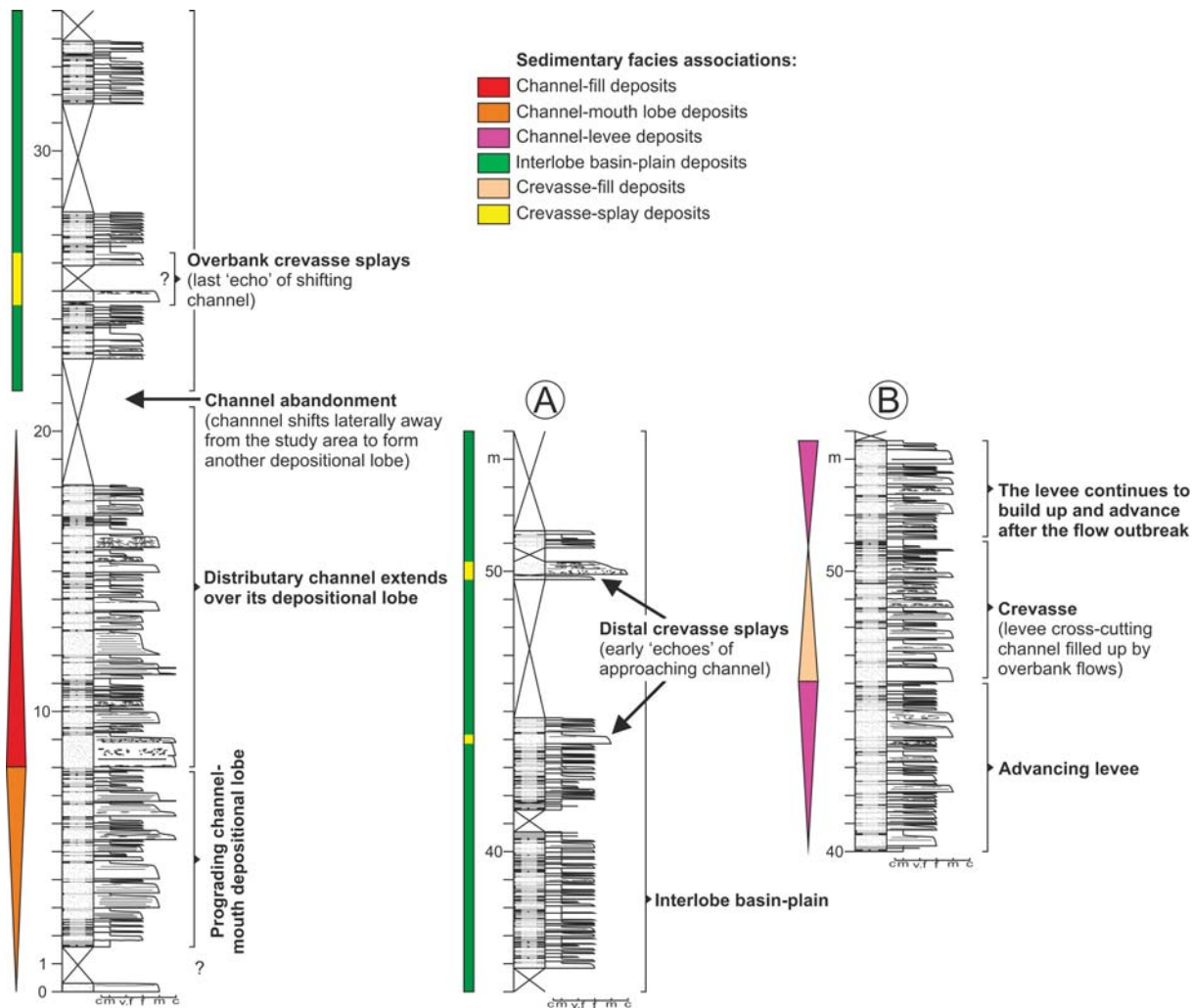
Text-fig. 12. Interpretation of the stratigraphic organization of facies associations in the Hucisko Jawornickie section (log segments A, B, C, E and G) in terms of morphodynamic evolution of the depositional system (Text-fig. 12 – continued on pp. 22–23)

nelized part of a similar earlier complex (described from another outcrop section by Łapcik 2017). The youngest, poorly exposed part of the succession (section segments H and I, Text-fig. 3) is dominated by mudstones, marlstones and mud-rich debrites and probably represents progradation of the basin-slope deposits over the base-of-slope sandy ramp system (*sensu* Reading and Richards 1994). The basinward advance of the whole system was terminated by a bulk deepening of the Skole Basin and its sediment-sourcing northern shelf zone, as indicated by the overlying Variegated Shale Formation of Paleocene–Eocene age (Text-fig. 2).

The base-of-slope system involved depositional lobes with leveed distributary channels and le-

vee-crossing crevasses, surrounded by interlobe basin plain with channel-derived crevasse splays (Text-fig. 11A). The progradational system was strongly aggrading, which caused intralobe lateral shifting of distributary channels by avulsion as well as a bulk lobe switching by upstream shifts of the local feeder conduit (Text-fig. 11B). The sedimentation history of the system recorded in the Hucisko Jawornickie outcrop section (Text-fig. 3) can be accordingly deciphered and interpreted from the upward organization of facies associations (Text-fig. 12).

The lowermost part of the stratigraphic succession (thickness interval 0–20 m of log segment A, Text-fig. 12), corresponding to the Wiar Member of the Ropianka Formation (Text-fig. 2), shows a pro-

A — **Channel levee** (heralding channel migration towards the study area, with subsequent shift back away)

Interlobe basin-plain sedimentation

B — Overbank splay

Overbank splay

Overbank splay

Overbank splay complex (multiple splays)

Overbank splay

Overbank splay

Overbank splays

Overbank splay complex

Overbank splay

Channel shifts closer the study area

Channel shifts away from the study area

Channel shifts closer the study area

Channel shifts abruptly away from the study area

Channel shifts closer the study area

Channel shifts away from the study area

Channel shifts closer to the study area

Interlobe basin plain with sand splays as an 'echo' of distributary channel shifting in adjacent lobe area

grading channel-mouth depositional lobe (base un-exposed) overlain erosively by its parental distributary channel. The channel then shifted laterally by avulsion, leaving a trailing record of crevasse splays (log A interval 20–30 m, Text-fig. 12) and delivering sand to another sector of the depositional lobe. The bulk aggradation caused an upstream shift of the feeder channel (cf. Text-fig. 11B), whereby the lobe was abandoned and turned into a basin plain (log A interval 30–90 m, Text-fig. 12), while an adjoining new depositional lobe was probably being formed. This new lobe's distributary channel only occasionally shifted sufficiently close to the study area to leave a record of levees (log A interval 90–98 m and log B interval 40–55 m, Text-fig. 12), but otherwise was shedding there only occasional crevasse splays according with its lateral shifting. The emplacement of crevasse splays in a quasi-abandoned study area (log B interval 55–100 m, Text-fig. 12) is an important 'echo record' of the distributary channel lateral shifting in the adjacent area of a new lobe deposition, consistent with the notion of avulsive distributaries.

The feeder channel eventually switched back to the study area, forming a new prograding depositional lobe overlain erosively by its distributary channel (log C interval 0–45 m, Text-fig. 12). The distributary channel shifted briefly sideways (log C top), but soon returned by avulsion to continue its lobe-building action (log E and interval 0–13.5 m of log G, Text-fig. 12). The overlying erosive package of sand-dominated deposits (log G interval 13.5–54 m, Text-fig. 12) is probably the local feeder valley that finally extended over the base-of-slope system and was filled with vertically stacked, amalgamated channel-fill deposits. The poorly exposed deposits in the topmost part of the outcrop succession (section segments H and I, Text-fig. 3), fine-grained and rich in muddy debrites, are attributed to an advance of the basin-slope deposits over the base-of-slope ramp system.

In terms of sequence stratigraphy (Catuneanu 2006; Helland-Hansen 2009), the sedimentary succession may be considered as representing a progradational normal-regressive lowstand systems tract, turning into an increasingly aggradational transgressive systems tract – when even the feeder valley was back-filled. The transgression culminated in the deposition of the Variegated Shale Formation (Text-fig. 2) at the highstand of relative sea level.

The sedimentation occurred during a long-term eustatic sea-level fall by about 15 m from the mid-Campanian to end-Maastrichtian (Haq 2014, fig. 4), which indicates that the coeval relative sea-level rise and transgression in the Skole Basin must have been caused by local tectonics. The early tectonic contraction of Carpathian orogen had probably both deepened and narrowed the basin, as indicated by a marked advance of the basin-margin slope. However, several short-term eustatic fluctuations on the order of 30–50 m occurred during the period of sedimentation (see 3rd-order eustatic cycles KCa3–KCa7 and KMa1–KMa5 in Haq 2014, fig. 4). Their potential impact on the depositional system behaviour is difficult to assess due to the sparsity of biostratigraphic data from the sedimentary succession, but it is quite possible that the system morphodynamic development was not controlled solely by autogenic processes. For example, the evidence of multiple lobe advances (log C, Text-fig. 12) and deeply erosional amalgamation of vertically stacked palaeochannels (log G, Text-fig. 12) might well indicate an influence of short-term eustatic changes. Eustatic fluctuations would have their greatest impact on the basin-margin shelf, which might explain the alternating supply of siliciclastic mud and calcareous mud (marl) as well as the episodic delivery of plant detritus and exotic gravel from the shelf zone.

IMPLICATIONS FOR THE SKOLE BASIN

Based on a detailed sedimentological analysis of available outcrop sections (Hucisko Jawornickie, Manasterz and Słonne, Text-fig. 1A), the depositional system of the Ropianka Formation is interpreted as a base-of-slope clastic ramp supplied with coarse sediment from the basin shelf zone through incised slope valleys (Text-fig. 13). The shelf was probably narrow and controlled by short-term eustatic fluctuations, with carbonate sedimentation dominant during sea-level highstands and with deltas reaching the shelf edge during lowstands. The occurrence of a mud-accumulating slope between the base-of-slope sandy ramp and the sediment-supplying shelf zone would explain why the Ropianka Formation is increasingly dominated by marlstone and mudstone facies towards its northerly source zone.

The lateral switching of depositional lobes (Text-fig. 11B) and temporal occupation of abandoned lobe areas by fine-grained basinal sedimentation may explain further the limited lateral extent of marlstone-and/or mudstone-dominated wedges within the Ropianka Formation. These wedges were recognized by surface mapping in the lower parts of the Cisowa, Wiar and Leszczyny members (Text-fig. 2), but the steeply folded and poorly exposed formation is likely
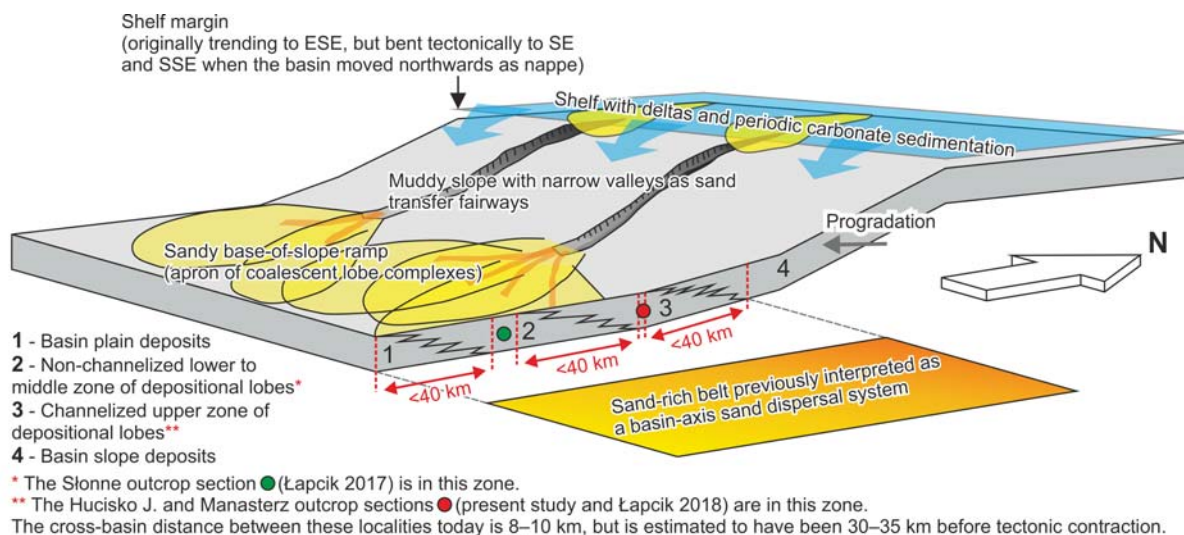
Text-fig. 13. Schematic conceptual model for the deposition of Ropianka Formation in the Skole Basin based on the Hucisko Jawornickie (present study), Manasterz (Łapcik 2018) and Słonne (Łapcik 2017) outcrop sections (see Text-fig. 1A)

to contain many more such thick local patches of fine-grained deposits (see Text-fig. 12, interval 20–100 m of log A and interval 54–100 m of log B). The hypothetical sedimentation model (Text-fig. 11) predicts that the main morphodynamic changes in the depositional system, such as lobe switching, were likely autogenic and non-synchronous, which would mean that the Ropianka Formation most probably lacks a simple layer-cake lithostratigraphy.

The channelized lobe complex studied in the Hucisko Jawornickie section, with a coeval feeder channel documented by Łapcik (2018) in the nearby Manasterz section, had prograded over the non-channelized distal part of an earlier similar lobe complex studied by Łapcik (2017) in the Słonne section (see section localities in Text-fig. 1A). The basinward distance between the Słonne section and the Hucisko Jawornickie section in the folded Skole Nappe is about 10 km (Text-fig. 1A), but is estimated to have been originally at least 35 km. If this estimate is correct, the basinward extent of the prograding base-of-slope ramp system would be around 100 km (Text-fig. 13), with the ramp evolving into a semi-continuous apron (*sensu* Reading and Richards 1994) by the lateral switching of depositional lobes and their coalescent vertical stacking. This sand-rich belt was indeed recognized by the earlier researchers from surface mapping, but was considered to represent a long-distance system of axial sand transport in the synclinal basin (e.g., Książkiewicz 1962; Bromowicz 1974; Kotlarczyk 1978). However, the measured local

sediment transport directions appeared to be highly varied and hardly supporting this interpretation, indicating transport mainly from the NW, N and NE (see Łapcik 2017, fig. 1A).

The present study and related studies by Łapcik (2017, 2018) have suggested a system of transverse, rather than longitudinal, sand dispersal and indicated that the system's feeder and distributary channels were quite small by global standards (Howell and Normark 1982; Clark and Pickering 1996; Clark and Gardiner 2000), unlikely to form depositional lobes more than 3–4 km in radial length. The high variation of local transport directions is fully compatible with the present model, taking into account the avulsive channel shifting, sideways building of levees, crevassing and lateral lobe switching (Text-fig. 11) and the ultimate tectonic bending and eastward rotation of the Skole Nappe (Text-fig. 1A). Features indicative of palaeotransport direction are seldom exposed even in such relatively good outcrops as the Hucisko Jawornickie section and may have little exact meaning without being linked to specific facies association.

CONCLUSIONS

This sedimentological study of the Wiar and Leszczyny members of deep-marine Ropianka Formation in the Hucisko Jawornickie outcrop section of Skole Nappe allowed distinction of seven com-

ponent sedimentary facies representing a range of sediment-gravity flows and episodes of hemipelagic to pelagic sedimentation with possible intervention of tidal or contouritic bottom currents. The stratigraphic grouping of sedimentary facies indicated six facies associations, interpreted as representing various morphodynamic architectural elements of a base-of-slope depositional system: distributary channels, channel-mouth lobes, channel levees, interlobe basin plain, crevasses and crevasse splays. The individual facies associations have been characterized in quantitative terms of statistics, and their internal modal organization of component facies has been studied and interpreted by using Markov chain analysis.

The stratigraphic succession in the Hucisko Jawornickie section is interpreted as a complex of channelized depositional lobes, with the vertical organization of facies associations reflecting chiefly autogenic morphodynamics of an aggrading base-of-slope system. The thick erosional package of amalgamated channel-fill deposits in the uppermost part of succession is interpreted as a basinwards extended and back-filled feeder valley, buried by muddy deposits of an advancing basin slope. The slope advance over the base-of-slope ramp culminated in a strong deepening of the Skole Basin and deposition of the Paleocene–Eocene Variegated Shale Formation. This dramatic change finds no explanation in coeval eustasy and is attributed to the basin tectonics. Short-term eustatic fluctuations are thought to have had a major impact on the basin's sediment-supplying shelf zone.

The base-of-slope sandy system of the Ropianka Formation is estimated to have comprised depositional lobes with a radial length of 30–40 km and to have prograded basinwards over a distance of around 100 km, while undergoing strong aggradation. The lateral switching of lobes and their coalescent vertical stacking resulted in a base-of-slope apron, which was recognized as a sand-rich belt by previous researcher from surface mapping, but was misperceived as an axial system of sand dispersal in the synclinal basin.

The present study, as the first detailed analysis of the Hucisko Jawornickie outcrop section, is a major contribution to the sedimentological understanding of the Ropianka Formation and the Late Cretaceous–Paleocene development in the Skole Basin. Last, but not least, this sedimentological case study demonstrates that a great deal of valuable information can be derived even from a single outcrop section of a poorly exposed sedimentary formation on the basis of detailed facies analysis conducted with appropriate methods.

REFERENCES

Alexander, J. and Morris, S. 1994. Observations on experimental, nonchannelized high-concentration turbidity currents and variations in deposits around obstacles. *Journal of Sedimentary Research*, **64**, 899–909.

Alexander, J. and Mulder, T. 2002. Experimental quasi-steady density currents. *Marine Geology*, **186**, 195–210.

Ashley, G.M., Southard, J.B. and Boothroyd, J.C. 1982. Deposition of climbing-ripple beds: a flume simulation. *Sedimentology*, **29**, 67–79.

Baas, J.H. 2004. Conditions for formation of massive turbiditic sandstones by primary depositional processes. *Sedimentary Geology*, **166**, 293–310.

Baas, J.H., Best, J.L., Peakall, J. and Wang, M. 2009. A phase diagram for turbulent, transitional, and laminar clay suspension flows. *Journal of Sedimentary Research*, **79**, 162–183.

Barwicz-Piskorz, W. and Rajchel, J. 2012. Radiolarian and agglutinated foraminiferal biostratigraphy of the Paleogene deep-water deposits on the northern margin of the Carpathian Tethys (Skole Unit). *Geological Quarterly*, **56**, 1–24.

Bayliss, N.J. and Pickering, K.T. 2015a. Transition from deep-marine lower-slope erosional channels to proximal basin-floor stacked channel-lévée-overbank deposits, and syn-sedimentary growth structures, Middle Eocene Banastón System, Ainsa Basin, Spanish Pyrenees. *Earth-Science Review*, **144**, 23–46.

Bayliss, N.J. and Pickering, K.T. 2015b. Deep-marine structurally confined channelised sandy fans: Middle Eocene Morillo System, Ainsa Basin, Spanish Pyrenees. *Earth-Science Review*, **144**, 82–106.

Bąk, K., 2007. Environmental changes around the Cenomanian–Turonian boundary in a marginal part of the Outer Carpathian Basin expressed by microfacies, microfossils and chemical records in the Skole Nappe (Poland). *Annales Societatis Geologorum Poloniae*, **77**, 39–67.

Bąk, K., Bąk, M., Górny, Z. and Wolska, A. 2014. Environmental conditions in a Carpathian deep-sea basin during the period preceding Oceanic Anoxic Event 2 – a case study from the Skole Nappe. *Geologica Carpathica*, **65**, 433–450.

Bernhardt, A., Jobe, Z.R. and Lowe, D.R. 2011. Stratigraphic evolution of a submarine channel–lobe complex system

in a narrow fairway within the Magallanes foreland basin, Cerro Toro Formation, southern Chile. *Marine and Petroleum Geology*, **28**, 785–806.

Best, J. and Bridge, J. 1992. The morphology and dynamics of low amplitude bedwaves upon upper stage plane beds and the preservation of planar laminae. *Sedimentology*, **39**, 737–752.

Breien, H., De Blasio, F.V., Elverhøi, A., Nystruen, J.P. and Harbitz, C.B. 2010. Transport mechanisms of sand in deep-marine environments – insights based on laboratory experiments. *Journal of Sedimentary Research*, **80**, 975–990.

Bromowicz, J. 1974. Facial variability and lithological character of Inoceramian Beds of the Skole-Nappe between Rzeszów and Przemyśl. *Prace Geologiczne*, **84**, 1–83. [In Polish with English summary]

Bouma, A.H. 1962. Sedimentology of Some Flysch Deposits: A Graphic Approach to Facies Interpretation, 168 pp. Elsevier; Amsterdam.

Bouma, A.H. 2000. Coarse-grained and fine-grained turbidite systems as end member models: applicability and dangers. *Marine and Petroleum Geology*, **17**, 137–143.

Bruhn, C.H.L. and Walker, R.G. 1997. Internal architecture and sedimentary evolution of coarse-grained, turbidite channel-levee complexes, Early Eocene Regência Canyon, Espírito Santo Basin, Brazil. *Sedimentology*, **44**, 17–46.

Brunt, R.L., Hodgson, D.M., Flint, S.S., Pringle, J.K., Di Celma, C., Prélat, A. and Grecula, M. 2013. Confined to unconfined: anatomy of a base of slope succession, Karoo Basin, South Africa. *Marine and Petroleum Geology*, **41**, 206–221.

Burzewski, J. 1966. Baculites marls on the lithostratigraphy background of the upper Inoceramian Beds of the Skiba Carpathians. *Zeszyty Naukowe AGH, Geologia*, **7**, 89–115. [In Polish with French summary]

Cantelli, A., Pirmez, C., Johnson, S. and Parker, G. 2011. Morphodynamic and stratigraphic evolution of self-channelized subaqueous fans emplaced by turbidity currents. *Journal of Sedimentary Research*, **81**, 233–247.

Carter, R.M. 1988. The nature and evolution of deep-sea channel systems. *Basin Research*, **1**, 41–54.

Catuneanu, O. 2006. Principles of Sequence Stratigraphy, 375 p. Elsevier, Amsterdam.

Clark, J.D. and Gardiner, A.R. 2000. Outcrop analogues for deep-water channel and levee genetic units from the Grès d'Annot turbidite system, SE France. In: Weimer, P., Slatt, R.M., Coleman, J.L., Rosen, N., Nelson, C.H., Bouma, A.H., Styzen, M. and Lawrence, D.T. (Eds), Global Deep-Water Reservoirs. Gulf Coast Section SEPM Foundation 20th Annual Bob F Perkins Research Conference, pp. 175–190. Houston.

Clark, J.D. and Pickering, K.T. 1996. Architectural elements and growth patterns of submarine channels: application to hydrocarbon exploration. *American Association of Petroleum Geologists Bulletin*, **80**, 194–220.

Collinson, J.D., Mountney, N.P. and Thompson, D.B. 2006. Sedimentary Structures, 292 p. Terra Publishing; Harpenden.

Crowell, J.C. 1957. Origin of pebbly mudstones. *Geological Society of America Bulletin*, **68**, 993–1010.

Davis, J.C. 2002. Statistics and Data Analysis in Geology, 638 p. John Wiley & Sons; New York. [3rd ed.]

Deptuck, M.E., Piper, D.J.W., Savoye, B. and Gervais, A. 2008. Dimensions and architecture of Late Pleistocene submarine lobes off the northern margin of East Corsica. *Sedimentology*, **55**, 869–898.

Deptuck, M.E., Sylvester, Z., Pirmez, C. and O'Byrne, C. 2007. Migration–aggradation history and 3-D seismic geomorphology of submarine channels in the Pleistocene Benin-major Canyon, western Niger Delta slope. *Marine and Petroleum Geology*, **24**, 406–433.

Dott, R.H., Jr. 1983. Presidential address: Episodic sedimentation – How normal is average? How rare is rare? Does it matter? *Journal of Sedimentary Petrology*, **53**, 5–23.

Drake, T.G. 1990. Structural features in granular flows. *Journal of Geophysical Research*, **B95**, 8681–8696.

Dykstra, M. 2012. Deep-water tidal sedimentology. In: Davis, R.A. and Dalrymple, R.W. (Eds), Principles of Tidal Sedimentology, pp. 371–396. Springer; Berlin.

Dżułyński, S. and Smith, A.J. 1964. Flysch facies. *Rocznik Polskiego Towarzystwa Geologicznego*, **34**, 245–266.

Ferry, J.N., Mulder, T., Parize, O. and Raillard, S. 2005. Concept of equilibrium profile in deep water turbidite system: effects of local physiographic changes on the nature of sedimentary process and the geometries of deposits. In: Hodgson, D.M., and Flint, S.S. (Eds), Submarine Slope Systems: Processes and Products. *Geological Society of London Special Publication*, **244**, 181–193.

Galloway, W.E. 1998. Siliciclastic slope and base-of-slope depositional systems: component facies, stratigraphic architecture, and classification. *American Association of Petroleum Geologists Bulletin*, **82**, 569–595.

Gardner, M.H., Borer, J.M., Melick, J.J., Mavilla, N., Dechesne, M. and Wagerle, R.N. 2003. Stratigraphic process-response model for submarine channels and related features from studies of Permian Brushy Canyon outcrops, West Texas. *Marine and Petroleum Geology*, **20**, 757–787.

Gągała, Ł., Vergés, J., Saura, E., Malata, T., Ringenbach, J., Werner, P. and Krzywiec, P. 2012. Architecture and orogenic evolution of the northeastern Outer Carpathians from cross-section balancing and forward modelling. *Tectonophysics*, **532–535**, 223–241.

Ge, Z., Nemec, W., Gawthorpe, R.L. and Hansen, E.W.M. 2017. Response of unconfined turbidity current to normal-fault topography. *Sedimentology*, **64**, 932–959.

Gedl, E. 1999. Lower Cretaceous palynomorphs from the Skole Nappe (Outer Carpathians, Poland). *Geologica Carpathica*, **50**, 75–90.

Gee, M.J.R., Masson, D.G., Watts, A.B. and Allen, P.A. 1999.

The Saharan debris flow: an insight into the mechanics of long runout submarine debris flows. *Sedimentology*, **46**, 317–335.

Geroch, S., Krysowska-Iwaszkiewicz, M., Michalik, M., Prochazka, K., Radomski, A., Radwański, Z., Unrug, Z., Unrug, R. and Wieczorek, J. 1979. Sedimentation of Węgierka Marls (Late Senonian, Polish Flysch Carpathians). *Annales Societatis Geologorum Poloniae*, **49**, 105–134. [In Polish with English summary]

Gradstein, F., Ogg, J., Schmitz, M. and Ogg, G. 2012. The Geological Time Scale 2012, 1176 p. Elsevier; Oxford.

Grundvåg, S.A., Johannessen, E.P., Hansen, W.H. and Plink-Björklund, P. 2014. Depositional architecture and evolution of progradationally stacked lobe complexes in the Eocene Central Basin of Spitsbergen. *Sedimentology*, **61**, 535–569.

Gucik, S. 1963. Profile of the Lower Cretaceous from Bełwin in the Przemyśl Carpathians. *Kwartalnik Geologiczny*, **7**, 257–268. [In Polish with English summary]

Gucik, S., Paul, Z., Ślączka, A. and Żytko, K. 1980. Mapa geologiczna Polski 1:200 000, arkusz Przemyśl, Kalników. Wydawnictwa Geologiczne; Warszawa. [In Polish]

Harms, J.C., Southard, J.B., Spearing, D.R. and Walker, R.G. 1975. Depositional Environments as Interpreted from Primary Sedimentary Structures and Stratification Sequences. Lecture Notes, SEPM Short Course No. 2, 161 p. Society of Economic Paleontologists and Mineralogists; Dallas.

Haughton, P.D.W., Davis, C., McCaffrey, W. and Barker, S.P. 2009. Hybrid sediment gravity flow deposits – classification, origin and significance. In: Amy, L.A., McCaffrey, W.B. and Talling, P.J. (Eds), Hybrid and Transitional Submarine Flows. *Marine and Petroleum Geology*, **26**, 1900–1918.

Haq, B.U. 2014. Cretaceous eustasy revisited. *Global and Planetary Change*, **113**, 44–58.

He, Y., Gao, Z., Luo, J., Luo, S. and Liu, X. 2008. Characteristics of internal-wave and internal-tide deposits and their hydrocarbon potential. *Petroleum Science*, **5**, 37–44.

Helland-Hansen, W. 2009. Towards the standardization of sequence stratigraphy: Discussion. *Earth-Science Review*, **94**, 95–97.

Heller, P.L. and Dickinson, W.R. 1985. Submarine ramp facies model for delta-fed, sand-rich turbidite systems. *American Association of Petroleum Geologists Bulletin*, **69**, 960–976.

Hodgson, D.M., Di Celma, C.N., Brunt, R.L. and Flint, S.S. 2011. Submarine slope degradation and aggradation and the stratigraphic evolution of channel–levee systems. *Journal of the Geological Society of London*, **168**, 625–628.

Hoffmann, M., Kołodziej, B. and Skupien, P., 2017. Micro-encruster-microbial framework and synsedimentary cements in the Štramberk Limestone (Carpathians, Czech Republic): Insights into reef zonation. *Annales Societatis Geologorum Poloniae*, **87**, 325–347.

Howell, D.G. and Normark, W.R. 1982. Sedimentology of submarine fans. In: Scholle, P.A. and Spearing, D.R. (Eds), Sandstone Depositional Environments. *American Association of Petroleum Geologists Memoir*, **31**, 365–404.

Hubbard, S.M., Romans, B.W. and Graham, S.A. 2008. Deep-water foreland basin deposits of the Cerro Toro Formation, Magallanes basin, Chile: architectural elements of a sinuous basin axial channel belt. *Sedimentology*, **55**, 1333–1359.

Hubbard, S.M., Covault, J.A., Fildani, A. and Romans, B.R. 2014. Sediment transfer and deposition in slope channels: Deciphering the record of enigmatic deep-sea processes from outcrop. *Geological Society of America Bulletin*, **126**, 857–871.

Ilstad, T., Marr, J.G., Elverhøi, A. and Harbitz, C.B. 2004. Laboratory studies of subaqueous debris flows by measurements of pore-fluid pressure and total stress. *Marine Geology*, **213**, 403–414.

Janbu, N.E., Nemec, W., Kırman, E. and Özaksoy, V. 2007. Facies anatomy of a channelized sand-rich turbiditic system: the Eocene Kusuri Formation in the Sinop Basin, north-central Turkey. In: Nichols, G., Paola, C. and Williams, E.A. (Eds), Sedimentary Environments, Processes and Basins – A Tribute to Peter Friend. *International Association of Sedimentologists Special Publication*, **38**, 457–517.

Janocko, M., Nemec, W., Henriksen, S. and Warchoł, M. 2013. The diversity of deep-water sinuous channel belts and slope valley-fill complexes. *Marine and Petroleum Geology*, **41**, 7–34.

Jurkiewicz, H. and Woiński, J. 1981. Mapa geologiczna Polski, 1:200 000, arkusz Mielec. Wydawnictwa Geologiczne; Warszawa. [In Polish]

Kędzierski, M. and Leszczyński, S. 2013. A paleoceanographic model for the Late Campanian–Early Maastrichtian sedimentation in the Polish Carpathian Flysch basin based on nannofossils. *Marine Micropaleontology*, **102**, 34–50.

Kerr, R.C. 1991. Erosion of a stable density gradient by sedimentation-driven convection. *Nature*, **353**, 423–425.

Klaucke, I. and Hesse, R. 1996. Fluvial features in the deep-sea: new insights from the glacigenic submarine drainage system of the Northwest Atlantic Mid-Ocean Channel in the Labrador Sea. *Sedimentary Geology*, **106**, 223–234.

Kneller, B.C. and Branney, M.J. 1995. Sustained high-density turbidity currents and the deposition of thick massive sands. *Sedimentology*, **42**, 607–616.

Kotlarczyk, J. 1978. Stratigraphy of the Ropianka Formation or of Inoceramian beds in the Skole Unit of the Flysch Carpathians. *Prace Geologiczne, Polska Akademia Nauk, Oddział w Krakowie, Komisja Nauk Geologicznych*, **108**, 1–75. [In Polish with English summary]

Kotlarczyk, J. 1988. A Guidebook of 59th PTG Congress in Przemyśl, 298 p. Wydawnictwa AGH; Kraków. [In Polish]

Kotlarczyk, J., Jerzmańska, A., Świdnicka, E. and Wiszniowska, T. 2006. A framework of ichtyofaunal ecostratigraphy of the Oligocene–Early Miocene strata of the Polish Outer

Carpathian Basin. *Annales Societatis Geologorum Poloniae*, **76**, 1–111.

Kováč, M., Plašienka, D., Soták, J., Vojtko, R., Oszczypko, N., Less, G., Ćosović, V., Fügenschuh, B. and Králiková, S. 2016. Paleogene palaeogeography and basin evolution of the Western Carpathians, Northern Pannonian domain and adjoining areas. *Global and Planetary Change*, **140**, 9–27.

Książkiewicz, M. (ed.) 1962. Geological Atlas of Poland. Fascicle, 13 – Cretaceous and Early Tertiary in the Polish External Carpathians. Instytut Geologiczny; Warszawa. [In Polish with English summary]

Leclair, S.F. and Arnott, R.W.C. 2005. Parallel lamination formed by high-density turbidity currents. *Journal of Sedimentary Research*, **75**, 1–5.

Leszczyński, S., Malik, K. and Kędzierski, M. 1995. New data on lithofacies and stratigraphy of the siliceous and fucoid marl of the Skole nappe (Cretaceous, Polish Carpathians). *Annales Societatis Geologorum Poloniae*, **65**, 43–62. [In Polish with English summary]

Leszczyński, S. and Uchman, A. 1991. To the origin of variegated shales from flysch of the Polish Carpathians. *Geologica Carpathica*, **42**, 279–289.

Leszczyński, S. 2003. Bioturbation structures in the Holovnia Siliceous Marls (Turonian–Lower Santonian) in Rybotycze (Polish Carpathians). *Annales Societatis Geologorum Poloniae*, **73**, 103–122.

Leszczyński, S. 2004. Bioturbation structures of the Kropivnik Fucoid Marls (Campanian–lower Maastrichtian) of the Huwniki — Rybotycze area (Polish Carpathians). *Geological Quarterly*, **48**, 35–60.

Lowe, D.R. 1982. Sediment gravity flows, II. Depositional models with special reference to the deposits of high-density turbidity currents. *Journal of Sedimentary Petrology*, **52**, 279–297.

Lowe, D.R. 1988. Suspended-load fallout rate as an independent variable in the analysis of current structures. *Sedimentology*, **35**, 765–776.

Lowe, D.R. and Guy, M. 2000. Slurry-flow deposits in the Britannia Formation (Lower Cretaceous), North Sea: a new perspective on the turbidity current and debris flow problem. *Sedimentology*, **47**, 31–70.

Lowe, D.R., Guy, M. and Palfrey, A. 2003. Facies of slurry-flow deposits, Britannia Formation (Lower Cretaceous), North Sea: implications for flow evolution and deposit geometry. *Sedimentology*, **50**, 45–80.

Łapcik, P. 2017. Facies heterogeneity of a deep-sea depositional lobe complex: case study from the Słonne section of Skole Nappe, Polish Outer Carpathians. *Annales Societatis Geologorum Poloniae*, **87**, 301–324.

Łapcik, P. 2018. Sedimentary processes and architecture of Upper Cretaceous deep-sea channel deposits: a case from the Skole Nappe, Polish Outer Carpathians. *Geologica Carpathica*, **69**, 71–88.

Łapcik, P., Kowal-Kasprzyk, J. and Uchman, A. 2016. Deep-sea mass-flow sediments and their exotic blocks from the Ropianka Formation (Campanian–Paleocene) in the Skole Nappe: a case study of the Wola Rafałowska section (SE Poland). *Geological Quarterly*, **60**, 301–316.

Malata, T. and Poprawa, P. 2006. Evolution of the Skole Subbasin. In: Oszczypko, N., Uchman, A. and Malata, E. (Eds), Rozwój paleotektoniczny basenów Karpat zewnętrznych, pp. 101–110. Institute of Geological Sciences, Jagiellonian University; Kraków. [In Polish with English abstract]

Marini, M., Salvatore, M., Ravnås, R. and Moscatelli, M. 2015. A comparative study of confined vs. semi-confined turbidite lobes from the Lower Messinian Laga Basin (Central Apennines, Italy): Implications for assessment of reservoir architecture. *Marine and Petroleum Geology*, **63**, 142–165.

Mayall, M., Jones, E. and Casey, M. 2006. Turbidite channel reservoirs – Key elements in facies prediction and effective development. *Marine and Petroleum Geology*, **23**, 821–841.

McCave, I.N. and Jones, K.P.N. 1988. Deposition of ungraded muds from high-density non-turbulent turbidity currents. *Nature*, **133**, 250–252.

McHargue, T., Prycz, M.J., Sullivan, M.D., Clark, J.D., Fildani, A., Romans, B.W., Covault, J.A., Levy, M., Posamentier, H.W. and Drinkwater, N.J. 2011. Architecture of turbidite channel systems on the continental slope: Patterns and predictions. *Marine and Petroleum Geology*, **28**, 728–743.

Miall, A.D. 1973. Markov chain analysis applied to an ancient alluvial plain succession. *Sedimentology*, **20**, 347–364.

Miall, A.D. 1978. Lithofacies types and vertical profile models in braided river deposits: a summary. In: Miall, A.D. (Ed.), Fluvial Sedimentology. *Canadian Society of Petroleum Geologists Memoir*, **5**, 597–604.

Mohrig, D., Ellis, C., Parker, G., Whipple, K. and Hondzo, M. 1998. Hydroplaning of subaqueous debris flows. *Geological Society of America Bulletin*, **110**, 387–394.

Mulder, T. 2011. Gravity processes and deposits on continental slope, rise and abyssal plains. In: Hüeneke, H. and Mulder, T. (Eds), Deep-Sea Sediments. Developments in Sedimentology, Vol. 63, pp. 25–148. Elsevier; Amsterdam.

Mulder, T. and Alexander, J. 2001. The physical character of subaqueous sedimentary density flows and their deposits. *Sedimentology*, **48**, 269–299.

Mutti, E. and Normark, W.R. 1987. Comparing examples of modern and ancient turbidite systems: problems and concepts. In: Leggett, J.K. and Zuffa, G.G. (Eds), Marine Clastic Sedimentology, pp. 1–38. Graham and Trotman; London.

Nakajima, T., Satoh, M. and Okamura, Y. 1998. Channel-levee complexes, terminal deep-sea fan and sediment wave fields associated with the Toyama Deep-Sea Channel system in the Japan Sea. *Marine Geology*, **147**, 25–41.

Nelson, C.H., Maldonado, A., Barber, J.H. & Alonso, B. 1991. Modern sand-rich and mud-rich siliciclastic aprons: alternative base-of-slope turbidite systems to submarine fans.

In: Weimer, P. and Link, M.H. (Eds), Seismic Facies and Sedimentary Processes of Submarine Fans and Turbidite Systems, pp. 171–190. Springer-Verlag; New York.

Nemec, W., Alçiçek, M.C. and Özaksoy, V. 2018. Sedimentation in a foreland basin within synorogenic orocline: Palaeogene of the Isparta Bend, Taurides, SW Turkey. *Basin Research*, **30**, 650–670.

Nemec, W. and Postma, G. 1991. Inverse grading in gravel beds. Abstracts IAS 12th Regional Meeting, p. 38. International Association of Sedimentologists; Bergen.

Nemec, W., Steel, R.J., Porębski, S.J. and Spinnangr, Å. 1984. Domba Conglomerate, Devonian, Norway: process and lateral variability in a mass flow-dominated, lacustrine fan-delta. In: Koster, E.H. and Steel, R.J. (Eds), Sedimentology of Gravels and Conglomerates. *Canadian Society of Petroleum Geologists Memoir*, **10**, 295–320.

Nescieruk, P., Paul, Z., Ryłko, W., Szymakowska, F., Wójcik, A. and Żytko. K. 1995. Mapa geologiczna Polski, 1:200 000, arkusz Jasło. Polska Agencja Ekologiczna; Warszawa. [In Polish]

Nichols, G. 2009. Sedimentology and Stratigraphy, 419 p. Wiley-Blackwell; Oxford. [2nd ed.]

Normark, W.R., Posamentier, H. and Mutti, E. 1993. Turbidite systems: state of the art and future directions. *Reviews of Geophysics*, **31**, 91–116.

Olszewska, B. and Szydło, A. 2017. Environmental stress in the northern Tethys during the Paleogene: a review of foraminiferal and geochemical records from the Polish Outer Carpathians. *Geological Quarterly*, **61**, 682–695.

Pickering, K.T., Corregidor, J. and Clark, J.D. 2015. Architecture and stacking patterns of lower-slope and proximal basin-floor channelised submarine fans, Middle Eocene Ainsa System, Spanish Pyrenees: An integrated outcrop–subsurface study. *Earth-Science Review*, **144**, 47–81.

Pickering, K.T., Hiscott, R.N., Kenyon, N.H., Ricci Lucchi, F. and Smith, R.D.A. 1995. Atlas of Deep Water Environments: Architectural Style in Turbidite Systems, 334 p. Chapman and Hall; London.

Piper, D.J.W. 1978. Turbidite muds and silts on deep sea fans and abyssal plains. In: Stanley, D.J. and Kelling, G. (Eds), Sedimentation in Submarine Canyons, Fans and Trenches, pp. 163–176. Dowden, Hutchinson and Ross; Stroudsburg, Pennsylvania.

Posamentier, H.W. and Walker, R.G. 2006. Deep-water turbidites and submarine fans. In: Posamentier, H.W. and Walker, R.G. (Eds), Facies Models Revisited. *SEPM (Society for Sedimentary Geology) Special Publication*, **84**, 397–520.

Postma, G., Nemec, W. and Kleinspehn, K.L. 1988. Large floating clasts in turbidites: a mechanism for their emplacement. *Sedimentary Geology*, **58**, 47–61.

Prélat, A., Covault, J.A., Hodgson, D.M., Fildani, A. and Flint, S.S. 2010. Intrinsic controls on the range of volumes, mor-

phologies, and dimensions of submarine lobes. *Sedimentary Geology*, **232**, 66–76.

Prélat, A., Hodgson, D.M. and Flint, S.S. 2009. Evolution, architecture and hierarchy of distributary deep-water deposits: a high-resolution outcrop investigation from the Permian Karoo Basin, South Africa. *Sedimentology*, **56**, 2132–2154.

Prior, D.B., Bornhold, B.D. and Johns, M.W. 1984. Depositional characteristics of a submarine debris flow. *Journal of Geology*, **92**, 707–727.

Rajchel, J. 1990. Lithostratigraphy of the Upper Paleocene and Eocene sediments from the Skole Units. *Zeszyty Naukowe AGH, Geologia*, **48**, 1–112. [In Polish with English summary]

Rajchel, J. and Uchman, A. 1998. Ichnological record of palaeoenvironment in the transgressive Miocene deposits of the Skole Unit in the Dubiecko region (SE Poland). *Przegląd Geologiczny*, **46**, 523–529. [In Polish with English summary]

Reading, H.G. and Richards, M. 1994. Turbidite systems in deep-water basin margins classified by grain size and feeder system. *American Association of Petroleum Ggeologists Bulletin*, **78**, 792–822.

Reineck, H.-E. and Singh, I.B. 1980. Depositional Sedimentary Environments, 549 p. Springer-Verlag; New York.

Ricci Lucchi, F. and Valmori, E. 1980. Basin-wide turbidites in a Miocene, over-supplied deep-sea plain: a geometrical analysis. *Sedimentology*, **27**, 241–270.

Salata, D. and Uchman, A. 2013. Conventional and high-resolution heavy mineral analyses applied to flysch deposits: comparative provenance studies of the Ropianka (Upper Cretaceous–Paleocene) and Menilite (Oligocene) formations (Skole Nappe, Polish Carpathians). *Geological Quarterly*, **57**, 649–664.

Salata, D. 2014a. Advantages and limitations of interpretations of external morphology of detrital zircon: a case study of the Ropianka and Menilite formations (Skole Nappe, Polish Flysch Carpathians). *Annales Societatis Geologorum Poloniae*, **84**, 153–165.

Salata, D. 2014b. Detrital tourmaline as an indicator of source rock lithology: an example from the Ropianka and Menilite formations (Skole Nappe, Polish Flysch Carpathians). *Geological Quarterly*, **58**, 19–30.

Shanmugam, G. 2006. Deep-Water Processes and Facies Models: Implications for Sandstone Petroleum Reservoirs. Handbook of Petroleum Exploration and Production, 5, 475 p. Elsevier; Amsterdam.

Shanmugam, G. 2008. Deep-water bottom currents and their deposits. In: Rebesco, M. and Camerlenghi, A. (Eds), Developments in Sedimentology, Vol. 60, pp. 59–81. Elsevier; London.

Shanmugam, G. 2016a. Submarine fans: A critical retrospective (1950-2015). *Journal of Palaeogeography*, **5**, 2–76.

Shanmugam, G. 2016b. Slides, Slumps, Debris Flows, Turbidity Currents, and Bottom Currents. Reference Module in Earth Systems and Environmental Sciences, 87 p. Elsevier online; https://doi.org/10.1016/B978-0-12-409548-9.04380-3.

Shanmugam, G. 2017. Contourites: Physical oceanography, process sedimentology, and petroleum geology. *Petroleum Exploration and Development*, **44**, 183–216.

Shanmugam, G. and Moiola, R.J. 1991. Types of submarine fan lobes: models and implications. *American Association of Petroleum Geologists Bulletin*, **75**, 156–179.

Stow, D.A.V. and Bowen, A.J. 1978. Origin of lamination in deep sea, fine-grained sediments. *Nature*, **274**, 324–328.

Stow, D.A.V. and Bowen, A.J. 1980. A physical model for the transport and sorting of fine-grained sediment by turbidity currents. *Sedimentology*, **27**, 31–46.

Stow, D.A.V. and Faugères, J.C. 2008. Contourite facies and the facies model. In: Rebesco, M., Camerlenghi, A. and Van Loon, A.J. (Eds), Contourite Research: A Field in Full Development. Developments in Sedimentology Vol. 60, pp. 223–256. Elsevier; London.

Stow, D.A.V. and Mayall, M. 2000. Deep-water sedimentary systems: new models for the 21st century. *Marine and Petroleum Geology*, **17**, 125–135.

Strzeboński, P. 2015. Late Cretaceous–Early Paleogene sandy-to-gravelly debris flows and their sediments in the Silesian Basin of the Alpine Tethys (Western Outer Carpathians, Istebna Formation). *Geological Quarterly*, **59**, 195–214.

Strzeboński, P., Kowal-Kasprzyk, J. and Olszewska, B. 2017. Exotic clasts, debris flow deposits and their significance for reconstruction of the Istebna Formation (Late Cretaceous–Paleocene, Silesian Basin, Outer Carpathians). *Geologica Carpathica*, **68**, 562–582.

Sumner, E.J., Amy, L. and Talling, P.J. 2008. Deposit structure and processes of sand deposition from a decelerating sediment suspension. *Journal of Sedimentary Research*, **78**, 529–547.

Ślączka, A. and Kaminski, M.A. 1998. A guidebook to excursions in the Polish Flysch Carpathians. *Grzybowski Foundation Special Publication*, **6**, 11–71.

Ślączka, A., Renda, P., Cieszkowski, M., Golonka, J. and Nigro, F. 2012. Sedimentary basin evolution and olistolith formation: The case of Carpathian and Sicilian region. *Tectonophysics*, **568–569**, 306–319.

Talling, P.J. 2013. Hybrid submarine flows comprising turbidity current and cohesive debris flow: deposits, theoretical and experimental analyses, and generalized models. *Geosphere*, **9**, 460–488.

Talling, P.J., Masson, D.G., Sumner, E.J. and Malgesini, G. 2012. Subaqueous sediment density flows: Depositional processes and deposit types. *Sedimentology*, **59**, 1937–2003.

Tripsanas, E.K., Piper, D.J.W., Jenner, K.A. and Bryant, W.R. 2008. Submarine mass-transport facies: new perspectives on flow processes from cores on the eastern North American margin. *Sedimentology*, **55**, 97–136.

Uchman, A., Malata, E., Olszewska, B. and Oszczypko, N. 2006. Palaeobathymetry of the Outer Carpathians Basins. In: Oszczypko, N., Uchman, A. and Malata, E. (Eds), Rozwój paleotektoniczny basenów Karpat zewnętrznych, pp. 83–102. Institute of Geological Sciences, Jagiellonian University; Kraków. [In Polish with English abstract]

Walker, R.G. 1984. General introduction: facies, facies sequences and facies models. In: Walker, R.G. (Ed.), Facies Models. *Geoscience Canada Reprint Series*, **1**, 1–9. [2nd ed.]

Wdowiarz, S. 1949. Structure géologique des Karpates marginales au sud-est de Rzeszów. *Biuletyn Państwowego Instytutu Geologicznego*, **11**, 1–39. [In Polish with French summary]

Woiński, J. 1994. Mapa geologiczna Polski, 1:200 000, arkusz Rzeszów. Polska Agencja Ekologiczna; Warszawa. [In Polish]

Wynn, R.B., Kenyon, N.H., Stow, D.A., Masson, D.G. and Weaver, P.P. 2002. Characterization and recognition of deep-water channel-lobe transition zones. *American Association of Petroleum Geologists Bulletin*, **86**, 1441–1462.